

MEASUREMENT OF ABSOLUTE f -VALUES
FOR IRON GROUP ELEMENTS

Thesis by

Graydon Dee Bell

In Partial Fulfillment of the Requirements

For the Degree of

Doctor of Philosophy

California Institute of Technology

Pasadena, California

1957

ACKNOWLEDGEMENTS

This research has been carried out under the supervision of Dr. Robert B. King. I wish to express my gratitude for his guidance in the experimental part of this project and for the generous assistance and encouragement he has given in the preparation of this thesis. I also wish to thank Dr. Paul M. Routly who gave valuable aid in much of the experimental work and reviewed many of the calculations involved in the final data.

Dr. Milford H. Davis was responsible for instruction in use of the apparatus at the beginning of this work; his continued interest in the project has been very helpful. Many useful suggestions from Dr. William R. Smythe have also been very much appreciated.

ABSTRACT

The preliminary results obtained with an atomic beam apparatus designed to measure absolute f -values for elements of the iron group were not in good agreement with results obtained by other techniques. In order to locate and eliminate sources of error in the atomic beam experiment, each assumption made in the development of this technique has been analyzed and tested. Experimental methods used in this analysis and the conclusions which resulted are discussed in some detail.

This thorough investigation of the experiment led to a number of modifications of the apparatus and improved techniques for making accurate measurements. These improvements and their effects upon the results are described.

Atomic beam measurements of absolute f -values for resonance lines in the spectra of Cu I, Mn I, Fe I, and Cr I are presented and compared with values obtained by other investigators. An experimental curve of growth for one line of each element has been determined and compared with the theoretical curve of growth. The good agreement obtained indicates that the atomic beam method gives results which vary with experimental conditions as the theory predicts.

Suggestions are given for further absolute f -value research using the atomic beam method.

TABLE OF CONTENTS

<u>PART</u>	<u>TITLE</u>	<u>PAGE</u>
I.	INTRODUCTION	1
II.	RESUME OF THEORY	7
III.	APPARATUS	17
	A. Light Sources	17
	B. Optical System	19
	C. Furnace Boats and Tubes	22
	D. Temperature Regulator	29
	E. Microbalance Damper	33
	F. Microbalance Pans	35
	G. Recorder Installation	36
	H. Microphotometer	37
IV.	EXPERIMENTAL ANALYSIS AND TECHNIQUES	39
	A. Scattered Light	39
	B. Beam Distribution	41
	C. Reflection of Atoms	47
	D. Impulse Forces	49
	E. Deposit Rate Measurements	55
	F. Calibration of Optical Pyrometer	60
	G. Continuum	64
	H. Equivalent Width Measurements	65
V.	RESULTS AND CONCLUSIONS	68
	A. Cu I	69
	B. Mn I	79
	C. Fe I	87
	D. Cr I	93
	E. Errors	99
	F. Summary	100
VI.	SUGGESTIONS FOR FURTHER RESEARCH	106
	A. Experimental Techniques	106
	B. Iron Group Elements	107
	C. Other Elements	109
VII.	APPENDIX: THEORY FOR MULTIPLE LIGHT BEAM	117

LIST OF TABLES

<u>TABLE</u>	<u>TITLE</u>	<u>PAGE</u>
I.	Impulse Force Measurements	51
II.	Data for Cu I, $\lambda 3247$	76
III.	Data for Mn I, $\lambda 4031$	85
IV.	Data for Fe I, $\lambda 3720$	91
V.	Data for Cr I, $\lambda 4254$	97
VI.	Absolute f-Values for Lines in Spectra of the Iron Group	101

LIST OF FIGURES

<u>FIGURE</u>	<u>TITLE</u>	<u>PAGE</u>
1.	Optical System	20
2.	Temperature Control Circuit	31
3.	Atomic Beam Distribution	46
4.	Cu I, $\lambda 3247$	78
5.	Hyperfine Structure of Mn I, $\lambda 4031$	82
6.	Mn I, $\lambda 4031$	86
7.	Fe I, $\lambda 3720$	92
8.	Cr I, $\lambda 4254$	98

I. INTRODUCTION

The strength of a spectral line formed by a vapor of atoms depends upon the number of atoms in the vapor capable of absorbing or emitting the line and upon the intrinsic probability that these atoms will make the proper transition. The transition probability can be expressed in terms of a constant called the absolute f -value for the transition. Experimentally determined absolute f -values are important for comparison with theoretically derived values but are even more useful for elements where theoretical calculations cannot be carried out. There are industrial applications for f -values, but the greatest demand for them at the present time comes in the field of astrophysics. Absolute f -values are indispensable in the study of relative abundances of the elements in the sun and stars, and these investigations in turn are of great importance as checks on theories concerning element synthesis and stellar evolution. An extensive project recently undertaken by Goldberg, Muller, and Aller at the University of Michigan to redetermine the abundances of some forty elements in the sun is critically dependent on absolute f -values, and, similarly, stellar compositions, such as that of Tau Scorpii recently investigated by Aller, Elste, and Jugaku, can best be determined by measurements involving absolute line strengths. For both of these investigations, uncertainties in the absolute f -values are the major obstacle to definite abundance

determinations, according to Dr. Goldberg. In this work most of the f -values have been obtained from theoretical estimates, since absolute f -values are known from laboratory measurements for only about 18 of the elements which are of astronomical interest and some of these measurements are not considered very reliable. Thus, a great deal of work yet lies ahead in absolute f -value determinations.

In spite of the need for absolute f -values, experimental measurements of these constants have been undertaken by few investigators. Consequently, accurate f -values, which in most cases can only be determined experimentally, are known for lines of relatively few elements. Among the experimental projects which have been reported, the research of A. S. and R. B. King is outstanding. Using a specially designed electric furnace, these men have been able to investigate the absorption lines of metallic elements and have reported relative f -values for many lines of Fe I and Ti I^(1,2) and for several other elements of the iron group. R. B. King has extended this work to absolute f -value measurements using an absorption tube method. In this method a pure sample of the element is introduced into a quartz tube, or cell, which is then evacuated. The tube is heated in a specially designed electric furnace which allows a light beam from a source producing a continuous spectrum to be passed through the heated tube. The temperature of the tube is accurately measured and from vapor pressure data the concentration of absorbing atoms is

determined. Total absorption measurements made on the lines produced by the vapor in the tube then allow absolute f -values for the lines to be calculated. Using this method, R. B. King has made absolute f -value measurements for lines of Cd I and Cu I⁽³⁾ and Fe I.⁽⁴⁾ Other experimental investigations of absolute f -values have included the work done on the resonance lines of Cr I and Ni I by Estabrook,^(5,6) using the absorption tube technique, and measurements made by Huldt and Lagerqvist⁽⁷⁾ on emission lines of Cr I and Mn I. Some theoretical values can be found in tables given by Bates and Damgaard⁽⁸⁾ and a tabulation of both absolute and relative f -values as they were known in 1950 is given in Landolt-Börnstein.⁽⁹⁾

More recently, Kopfermann and Wessel^(10,11) developed an atomic beam method for absolute f -value measurements; they have reported absolute f -values for the resonance lines of Ba I and Fe I. Since the values for Fe I obtained by this method do not agree with those measured by the absorption tube technique, a similar atomic beam experiment was begun some time ago by R. B. King. Under his supervision the project was carried to the point of giving preliminary results by M. H. Davis⁽¹²⁾ and P. M. Routly.

In this experiment a sample of the element to be investigated is placed in a small, cylindrical crucible, called a boat, which then fits inside a thin-walled tube made of graphite or other conducting materials. This tube

is held in a horizontal position by water cooled electrodes and acts as the heating element of an electric furnace. A small hole in the wall of the boat and a somewhat larger hole in the heating tube allow atoms of the sample in the boat to emanate upward in a three dimensional, fan-shaped beam when the boat is heated to temperatures which cause evaporation of the sample. The atomic beam is formed in a vacuum chamber where a pressure of 10^{-4} to 10^{-5} mm. of mercury is maintained. Quartz windows in opposite sides of the vacuum chamber allow a light beam from a source which produces a continuous spectrum to pass through the atomic beam in the form of a narrow, thin sheet lying in a horizontal plane. The resonance lines of the sample are formed in absorption by the atomic beam and are photographed with a high dispersion spectrograph. Microphotometer tracings of the photographic plates are then used to determine the equivalent widths (or total absorption) of the absorption lines. At the same time the lines are being photographed, a direct measure of the concentration of atoms in the beam is made. This is accomplished by allowing a portion of the atomic beam to deposit on the pan of a very sensitive microbalance located directly above the atomic beam source. The rate at which this deposit increases with time can be used to calculate the density of atoms at any point in the beam, since the density distribution of atoms across the beam is known. The portion of the beam which strikes the microbalance pan is defined by a circular opening in a

horizontal plate which is located above the region through which the light beam passes. The temperature of the enclosure from which the atoms effuse is measured with an optical pyrometer, and dimensions such as the shape of the atomic beam and the height of the light beam above the orifice in the boat are measured directly with a micrometer. These quantities then enter into an equation which can be solved for the absolute f -value of the transition which produces the spectral line.

The atomic beam method, though not as simple in practice as in theory, provides a way of making absolute f -value determinations that is independent of vapor pressure data and does not require a highly accurate temperature determination. Measurements made by this method can be used to check those of other methods which have been applied to the same elements. Also, results by the atomic beam procedure can be obtained in some cases where the absorption tube method cannot be applied because vapor pressure data are not available.

Since the preliminary results for the resonance lines of Cu I, Fe I, Cr I, and Mn I obtained by Davis appeared low, and also showed considerable scatter, it seemed advisable to re-analyze the experiment in as much detail as possible and to improve the experimental techniques before proceeding to measurements on other elements of astronomical interest. Results of this analysis, modifications of

the apparatus, and improved techniques will be described in detail in Sections III and IV. First, however, a resume of the theory used in reducing the experimental data will be given.

II. RESUME OF THEORY

The absolute f-value or oscillator strength for an atomic transition from one energy state to another relates the number of atoms in the initial state to the number of transitions to the final state. It is a constant for a given transition and is proportional to the transition probability which, for the hydrogen atom at least, can be theoretically calculated. Such calculations, however, involve the matrix elements connecting the two energy states between which the transition occurs, and for complex atoms the wave functions needed to evaluate these matrix elements are not known. Thus, an experimental determination is often the only way of obtaining the absolute f-values which are needed for the applications mentioned in the previous section.

In order to derive f-values from experimental measurements on absorption or emission lines produced in a vapor of atoms, a relation between the strength of the line and other measurable parameters, such as the density of atoms in the vapor, must be known. As the density of atoms in a vapor increases, the total absorption for a spectral line produced by these atoms increases. A measure of the total absorption is best made in terms of the equivalent width of the line, since this quantity is not affected by the folding of the natural shape of the absorption line with the "window curve" of the spectrograph. The equiva-

lent width is customarily expressed in Angstrom units and is the effective wave length interval completely removed from a beam of continuous light by the absorbing atoms. For very weak absorption lines the relation between the density of atoms and the equivalent width of the line is a linear one. However, as the line becomes stronger it begins to "saturate" and the relation between the density of atoms and the equivalent width becomes more complicated. A logarithmic plot of the equivalent width of the line versus the number of atoms producing the line is called a "curve of growth."

In the case of pure doppler broadening, the relation between equivalent width and number of atoms can be expressed mathematically in the form of a series, and the theory can be extended to cover cases in which natural damping and pressure broadening are important. Derivations and discussions of these relations are given in books by Unsold⁽¹³⁾ and by Aller,⁽¹⁴⁾ and a good summary concerning the curve of growth is given in a thesis by Hill.⁽¹⁵⁾

Absorption lines produced in an atomic beam such as the one used for this experiment also follow a curve of growth which can be expressed mathematically in the form of a series similar to that referred to above. A straightforward derivation of this series for the atomic beam has been carried out by Davis and is given in detail in his thesis.⁽¹²⁾ This derivation is based on the following assumptions:

1. The density and velocity distribution functions for the atoms in the beam may be derived from the equations of kinetic theory of gases which describe molecular effusion.

2. The orifice from which the atoms emanate is sufficiently small to be considered a point source.

3. Collisions of atoms in the beam with each other and with residual gas molecules can be neglected.

4. All atoms in the beam stick to the cool surfaces of the apparatus and in particular to the pan of the microbalance.

These assumptions have been discussed by Davis in considerable detail, but they are repeated here since some of the experimental checks to be described in Section IV were carried out in order to determine their validity.

On the basis of these assumptions, Davis has derived a relation between the equivalent width, W , of an absorption line and a quantity C , which is essentially NfL , that is, the concentration of effective atoms in the atomic beam multiplied by the absolute f -value and by the length of the light beam path through the atomic beam. This relation is

$$\frac{W}{\Delta \lambda'_D} = \frac{W}{\Delta \lambda_D \sin \gamma} = \sqrt{\pi} \sum_{n=1}^{\infty} \frac{C^n (-1)^{n+1}}{n! \sqrt{n}} \quad (1)$$

where

W is the equivalent width measured in Angstrom units,

$\Delta\lambda_0$ is the doppler width measured in Angstrom units,

and

γ is the half-angle of the atomic beam.

The doppler width of the line is given by

$$\Delta\lambda_D = \frac{\lambda_0}{c} \sqrt{\frac{2RT}{M}} = 4.30 \times 10^{-4} \lambda_0 \sqrt{\frac{T}{M}} \quad (2)$$

where

λ_0 is the wave length of the center of the line in units of 10^{-5} cm.,

c is the velocity of light,

R is the gas constant per mole,

T is the absolute temperature, and

M is the atomic weight.

The quantity C is a function of the f -value and various parameters which are measured in the apparatus. This relation is

$$C = \frac{e^2}{2Rmc} M \frac{\lambda_0}{z_0} \frac{\rho^2 + b^2}{\rho^2} \frac{G'}{T} f \quad (3)$$

where

e is the charge on the electron,

m is the mass of the electron,

z_0 is the height of the light beam above the atomic beam source,

r is the radius of the circular opening which defines the deposit on the balance pan,
 b is the height of this opening above the source,
 G' is the deposit rate measured in atoms per second,
and
 f is the absolute f -value.

As an aid in making calculations, the many factors of this expression are combined into the relation

$$C = \frac{G}{QT} f \quad (4)$$

where

G is the deposit rate measured in micrograms per second, and

Q is a constant for any one run given by

$$Q = \frac{2Rmc}{e^2} \frac{1.66 \times 10^{-8} M}{M} \frac{Z_0}{\lambda_0} \frac{r^2}{r^2 + b^2}$$
$$Q = 3.28 \times 10^{-3} \frac{Z_0}{\lambda_0} \frac{r^2}{r^2 + b^2} \quad (5)$$

The factor $1.66 \times 10^{-8} M$ has been introduced here in order to convert G (the deposit rate measured in micrograms per second) to G' (the deposit rate in atoms per second).

The observed deposit rate, G , should be corrected for a Boltzmann distribution over energy levels other than the particular level from which the absorption line arises,

but this correction is generally negligible when the ground state is simple. When the ground state is not simple, as in the case of the a^5D state of Fe I, this correction is very important. The factor by which G should be multiplied is equal to the ratio of atoms, N_i , in the state from which the transition arises to the total number of atoms, N_T , in all states, and it is given by

$$\frac{N_i}{N_T} = \frac{g_i e^{-E_i/kT}}{\sum_j g_j e^{-E_j/kT}} \quad (6)$$

where

g_i is the statistical weight of the i th energy state,

i.e. $2J_i + 1$,

E_i is the energy of the i th state, and

k is Boltzmann's constant.

The relation given in equation 1 has been derived by Davis for a single traversal by the light beam, but it needs only a simple modification to make it applicable to experiments in which multiple traversals are used. To a very good approximation, the only change required is to replace the expression given for Q in equation 5 by

$$Q = 3.28 \times 10^{-3} \frac{\rho^2}{\rho^2 + b^2} \frac{1}{\lambda_0} \frac{1}{\frac{1}{z_1} + \frac{1}{z_2} + \dots + \frac{1}{z_1} + \dots + \frac{1}{z_n}} \quad (7)$$

where z_1 is the height of the light beam in its i th traversal above the orifice acting as the atomic beam source. Actually, every even numbered traversal of the light beam passes through the atomic beam at a small angle of inclination rather than horizontally, but this introduces a negligible effect as the derivation of equation 7 shows (see Appendix).

Only one further correction need be considered before equations 1 and 4 can be used to yield an absolute value for f . When the absorption line under consideration exhibits hyperfine splitting which is larger than the doppler width of the components but which is unresolved by the spectrograph, the equivalent width of the line should be divided into parts corresponding to the relative intensities of the components. A value of C is then determined for each part and these values are added together to give the total C for the line. This procedure is described in King's article⁽³⁾ on the absolute f -values for the resonance lines of Cu I and examples of it will be found here in the sections giving results for Cu I and Mn I.

To summarize then, the following relations are used in making absolute f -value calculations:

$$\frac{W}{\Delta \lambda'_D} = \frac{W}{\Delta \lambda_D \sin \gamma} = \sqrt{\pi} \sum_{n=1}^{\infty} \frac{C^n (-1)^{n+1}}{n! \sqrt{n}} \quad (8)$$

$$\Delta \lambda_0 = 4.30 \times 10^{-4} \lambda_0 \sqrt{\frac{T}{M}} \quad (9)$$

$$Q = 3.28 \times 10^{-3} \frac{f^2}{f^2 + b^2} \frac{1}{\lambda_0} \frac{1}{\frac{1}{z_1} + \frac{1}{z_2} + \dots + \frac{1}{z_n}} \quad (10)$$

$$f = \frac{C}{G/QT} \quad (11)$$

Equation 8 has been solved numerically with the aid of a computing machine and from tabulated results it yields values of C for given values of $W/\Delta\lambda_D$, the hyperfine splitting having been taken into account by the previously described procedure. The value of Q is calculated from quantities measured in the apparatus; it remains constant for all runs made on a given element so long as the optical system is left unchanged. The above expression for Q reduces to the simpler form given by equation 5 when a single beam is used. Quantities G and T are measured during the course of the run by methods to be described in the following section, and thus all quantities in equation 11 are known except the absolute f-value, f.

Though an absolute f-value can be calculated for each photographic exposure of the absorption line, an accumulation of data from a number of runs can be put into graphical form which then yields an average f-value. This is done by plotting $\log W/\Delta\lambda_D$ versus $\log G/QT$. Such a plot develops an experimental curve of growth which can then

be fitted to the theoretical curve given by equation 8. Since the relation between $W/\Delta\lambda_D$ and G/QT also involves $(\sin \gamma)^{-1}$ and f (see equations 8 and 11), a fit of the experimental curve to the theoretical curve ($\log W/\Delta\lambda_D$ vs. $\log C$) can be obtained only after a vertical shift equal to $+\log \sin \gamma$ and a horizontal shift equal to $-\log f$ have been made. This fitting of the experimental and theoretical curves not only yields an average value for f , as determined by the horizontal shift, but also provides a good test of the theory in cases where the knee of the experimental curve is well defined. If the knee of the experimental curve could best be fitted with the knee of the theoretical curve by a vertical shift of some factor not equal to $+\log \sin \gamma$, this would indicate that the theory did not provide the exact relation describing the curve of growth. In the course of experiments to be described later in this thesis, however, it became evident that the features of the atomic beam have been correctly analyzed by the theory and that a vertical shift in the graphs equal to $+\log \sin \gamma$ does allow a good fit to be obtained when only an additional horizontal shift is made. This important fact was most strikingly brought out in the case of Cu I (see Fig. 4). Graphical representations of the data for other elements have been made in order to further check this question and also to provide an average f -value when the data from many runs show considerable scatter.

As a last theoretical consideration, an expression is needed for the force acting on the microbalance due to the transfer of momentum as the atoms hit and stick to the balance pan. Such an expression involves only the deposit rate, the absolute temperature, and the atomic mass, that is,

$$F = \frac{3\sqrt{\pi}}{4} \sqrt{\frac{2RT}{M}} G \quad . \quad (12)$$

A derivation of this simple equation is given by Davis.⁽¹²⁾ Since both the observed force, F , and the deposit rate, G , are measured by the microbalance, the spring constant for the balance, which is generally needed in order to convert microbalance divisions to micrograms, cancels out of this equation. The importance of this impulse force is made obvious in Section IV D.

III. APPARATUS

The basic apparatus for the f-value measurements reported here has been described in detail by Davis.⁽¹²⁾ Various modifications of and additions to this apparatus have been made, however, and these are described in the following sections.

A. Light Sources

For the study of most elements, a high pressure mercury arc lamp operated by an alternating current of about 1 ampere at a voltage of around 1000 volts was used. This lamp operates with the capillary in a horizontal position and is cooled by a continuous flow of tap water through its quartz water jacket. The pressure broadened mercury lines form a very satisfactory continuum for the atomic beam absorption lines over a wide region of the ultra-violet and visible spectrum.

In the case of Mn I, however, the strongest lines (λ 4031, 4033, 4034) fall very close to a strong mercury line (λ 4047). Hence, the intensity of the "continuum" in this region changes so rapidly with wave length that accurate equivalent width measurements cannot be made. A high pressure xenon arc lamp provides a uniform continuum in this region but presents other difficulties because of its design. The xenon lamp is manufactured by the Osram Kommanditgesellschaft in Germany and operates without liquid

cooling on an alternating current of about 8 amperes at 220 volts. A starter circuit, which impresses a high voltage across the electrodes for a brief time, is incorporated into the power supply unit. The quartz envelope has the shape of a round bulb in which the sharply tapered electrodes are located with a separation of about 3 millimeters. The manufacturer specifies that this lamp should be operated in a vertical position, but in order to obtain most easily the horizontal sheet of light needed for this experiment the lamp was operated in a horizontal position. In this position the top of the bulb became gradually blackened, but the lamp gave a usable, stable discharge for many hours.

The chief objection to the xenon lamp for this experiment is that at the tip of each electrode the discharge is considerably brighter than in the region between the two electrodes. When this source is imaged on the slit of the spectrograph, the two bright spots produce streaks along the continuum. Such a difficulty can be minimized by measures described in Section IV G, but then the effective intensity of this source is too low to allow the short exposures of 30 seconds or less generally used with the mercury lamp. Nevertheless, this lamp was used satisfactorily in the work on manganese and it may prove useful again in the study of other elements.

B. Optical System

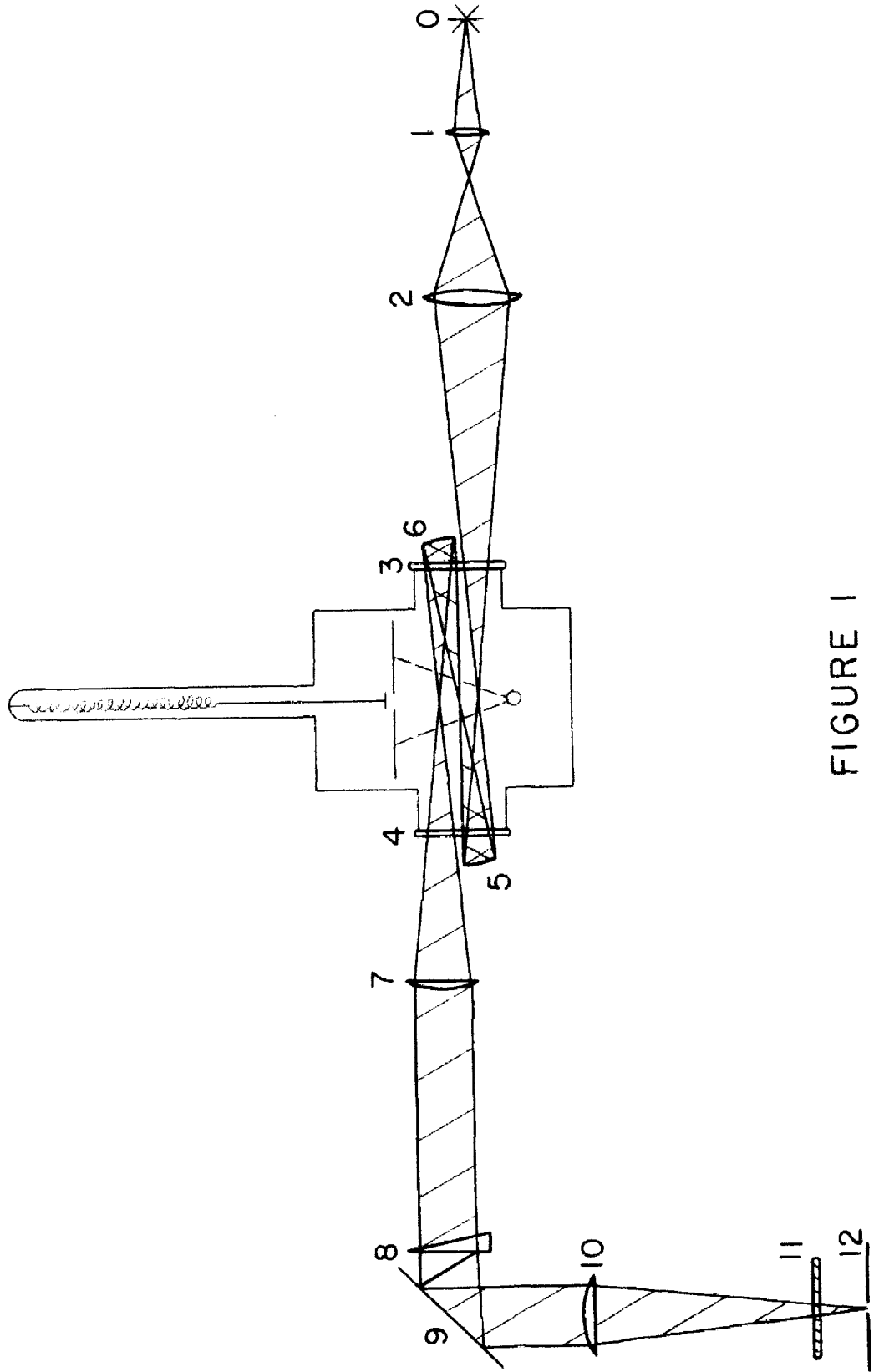
A schematic drawing of the optical system is given in Figure 1. Elements 1, 2, 7, and 10 of this system are quartz lenses with the following specifications:

<u>Number</u>	<u>Type</u>	<u>Diameter</u>	<u>Focal Length</u>
1	Achromat	2.5 cm.	+ 5.0 cm.
2	Double-convex	10.0 cm.	+ 15.0 cm.
7	Plano-convex	8.5 cm.	+ 60.0 cm.
10	Plano-convex	8.0 cm.	+ 40.0 cm.

Lens number 2 has been masked to a 3.0 cm. diameter since its full aperture is not needed to fill the grating. Lens number 10 is mounted on a movable rack which is engaged by a pinion gear in order that a smooth, horizontal to-and-fro motion of the lens covering a maximum displacement of 7 cm. can be made. This motion of the lens is provided manually during the photographic exposures in order to track the image of the light source back and forth along the slit. The need for this tracking of the image will be discussed in Section IV G.

Elements 5 and 6 of the optical system are small, concave mirrors which are inserted when three traversals by the light beam are desired. This arrangement will be referred to as a "triple beam" throughout this thesis. The mirrors were made from a specially ground plano-concave lens cut into two parts along a diameter and then coated

OPTICAL SYSTEM



120-

FIGURE 1

with aluminum. Each mirror has a focal length of 11.6 cm. and the two are separated by a distance of 46.4 cm. This separation locates the center of curvature for each mirror on the vertical axis of the furnace, and since the light beam is originally focused on this axis each mirror re-focuses the reflected beam there.

Elements 3 and 4 are the flat, quartz windows of the furnace and element 9 is a plane, aluminized glass mirror used to turn the beam from a horizontal to a vertical direction.

Element 8 is a small-angle, quartz foreprism. This prism disperses the light beam in wave length so that the image focused on the spectrograph slit is spread into a short spectrum which crosses the slit. The slit then passes only a short region of the spectrum, that is, the foreprism and slit together act as a monochromator. Prisms with angles of 10° , 20° , and 30° have been used for this purpose, but of these the 20° prism seems most satisfactory. For light in the wave length region of 4030 Angstroms, this prism has an angular dispersion of 4.04×10^{-6} radians per Angstrom and spreads a range of 1000 Angstroms into a band which is approximately 1.6 mm. long across the slit of the spectrograph. If such a spectrum were formed by an infinitely narrow source, it would allow a spectral band of about 25 Angstroms to enter the spectrograph, but due to the finite size of the source and various aberrations of the optics, the pass amounts to an effective range of some 100

Angstroms. The figures given here are based on calculations made for the wave length region of interest in the study of manganese, but the size of the pass is very nearly the same for wave length regions between 3200 and 4200 Angstroms. The need for this foreprism arrangement will be made obvious in Section IV A.

Element 11 of the optical system is a Packard shutter of $2\frac{1}{4}$ inches aperture operated by an a.c. solenoid connected to a "Time-O-Lite" electric timer. This allows uniform exposures ranging from 1 to 60 seconds to be made with an estimated variation of less than 0.1 second.

Element 12 is the slit of the spectrograph.

C. Furnace Boats and Tubes

As mentioned in Section I, the special crucible used to hold the element while it is being evaporated is called a boat. The boat is located at the center of a thin-walled tube through which an electric current is passed to cause heating. The graphite boats and graphite tubes described by Davis were used for all runs made on copper since this element shows no tendency to combine with the graphite. Molten copper, in fact, does not even wet the graphite but forms a spherical ball which vaporizes smoothly and uniformly. Chromium also can be vaporized from a graphite boat so long as the melting point is not exceeded, but runs were made in boats of other materials in an attempt to reduce the sputtering characteristic of this element.

Molten iron, on the other hand, combines so readily with the graphite that temperatures in excess of 1900° C. were required to produce even a weak atomic beam from a graphite boat. To attain such temperatures with the present apparatus, it was necessary to overload the transformer which delivers current to the furnace tube and to endanger some parts of the furnace with overheating. The accuracy with which temperatures in this range can be measured with an optical pyrometer is considerably less than at lower temperatures. Moreover, at these high temperatures the Boltzmann distribution over higher sub-levels of the a^5D state tends to reduce the relative number of iron atoms in the a^5D_4 ground state. Worse than this, the iron sample is so rapidly taken up by the graphite in the formation of iron carbide that it is practically impossible to maintain a constant beam for any length of time. And finally, it is impossible to produce the strong lines needed to develop a full curve of growth when the atomic beam is suppressed by the formation of iron carbide. For these reasons boats made of other materials had to be developed.

Davis used with some success a graphite boat lined with tantalum carbide. Such a boat when heated in a graphite tube produces a usable beam at temperatures above 1700° C. provided the hole from which the beam emanates is quite large, that is, roughly 1.5 mm. or more in diameter. Even so, the tantalum carbide is attacked by the molten

iron, and so much of the iron sample is lost through the liner and through combination with graphite subliming from the boat and tube as to make the maintenance of a strong, constant beam very difficult. For this reason tantalum carbide lined boats were abandoned after the first four runs on iron, but they were used quite effectively for all runs on manganese and for most of the runs on chromium.

In an effort to develop a boat which would combine in no way with the molten iron, attention was turned to such materials as zirconium oxide and thorium oxide. When these compounds are sintered by heating at high temperatures for long periods of time, they form very hard, strong structures which act as ideal crucibles for molten metals. Some attempts were made to press the dry powders of these oxides into the required shape, but due to the small size and thin walls of the boat the extreme pressures required in this process could not be applied.

At the suggestion of Dr. H. V. Neher, the process of molding these materials in a paste form was tried. This process was found to be feasible but difficult. At first, ordinary flour mixed with water was used as a binder. When zirconium oxide powder was added to this mixture, a thick paste was formed which could be cast in the shape of a short tube closed at one end. While still in the mold, this piece was warmed until dry in an oven at 95° C. The open end was then fitted with a plug machined from a piece of the same material, and a small hole was drilled in the side

to act as an orifice for the beam. Next, the boat was heated in an air atmosphere to a bright red heat which burned away all of the flour. Finally, it was placed in the furnace tube of the atomic beam apparatus and sintered. For zirconium oxide this sintering process requires a temperature in excess of 2000° C. and the compound should be held at temperatures in this range for at least 30 minutes, preferably for several hours.

A furnace tube made of graphite was first used as the heating element during the sintering process, but this reduced the zirconium oxide to a carbide which was undesirable as a crucible for molten iron. A furnace tube made of molybdenum was then tried and in this the zirconium oxide was sintered into a hard, strong form with only a thin coating of molybdenum on the outside. The shrinkage during sintering amounted to almost 30 percent.

Several boats were successfully made in this way, but the procedure possessed a number of disadvantages. First, air bubbles in the paste often left holes in the boat. Second, the boat often cracked during the drying process or broke as it was being removed from the mold. Smearing the mold with silicon stopcock grease abated but did not eliminate this difficulty. Third, the drying process required a period of at least 24 hours because almost none of the boat was actually exposed to the air while it was in the mold. Attempts to remove the boat from the mold before drying was complete invariably failed.

Some improvement in the process was attained by first cooking the mixture of flour and water in a double boiler until a jellied consistency was obtained. When this material was used as a binder, it gave more strength to the structure during the stage before sintering.

In an attempt to avoid cracking by thermal shock during the sintering process, zirconium oxide mixed with calcium oxide (so-called "stabilized zirconium oxide") was tried. This mixture, however, takes on a gritty consistency when mixed with water and cannot be molded easily. Also, this mixture is objectionable from the standpoint of possibly introducing calcium atoms into the atomic beam. Attempts to make boats of thorium oxide were not successful because this compound does not form a good suspension in water and is very difficult to mold.

A somewhat superior method was finally developed for forming the zirconium oxide boats. In this procedure the zirconium oxide powder and a small amount of the cooked flour are mixed with just enough water to form a thick paste which will hold its shape. This is then extruded through a 1 inch hole in a steel block, forming a round rod of the thick paste. The rod is then cut into short lengths which are dried in the oven with low heat.

When dry the short rods of zirconium oxide can be placed in the collet of a lathe and turned down to the required outside diameter. A straight flute drill is used to bore out the rod leaving a thin-walled tube with one

closed end. The small hole for the beam orifice is then drilled and finally the open end is plugged with a snugly fitting piece of the same material turned on a lathe to fit. The binder is burned away and the boat is sintered as before.

This extrusion process for the formation of zirconium oxide boats has the following advantages: the difficult molding process is eliminated; the drying process is much faster and shrinkage during this time merely decreases the diameter without causing cracks; machining on the lathe removes all surface flaws leaving a more solid and smooth outer surface; and the bore can be fitted with a plug more effectively than a molded hole.

Some preliminary experiments indicate that the sintering process can be improved by using an induction furnace instead of the atomic beam apparatus. If the zirconium oxide is heated in an air atmosphere, it is not reduced by carbon. Thus, a graphite heating element can be used. The graphite gradually burns away at the temperatures needed to sinter the zirconium oxide, but a thick-walled graphite crucible will survive for a sufficient time to complete the sintering process. A series of radiation shields made of alundum can be used to decrease radiation losses, and temperatures in excess of 2000° C. can be obtained with a 15 kilowatt furnace. The chief difficulty connected with this method for sintering lies in heating the boats slowly

and uniformly. If the temperature is changed too rapidly or if the boat is heated non-uniformly, it invariably cracks. Nevertheless, induction heating has several advantages over the other kind, and it can no doubt be perfected through further research.

The molybdenum tubes used for sintering in the atomic beam furnace were made from 0.0035 inch sheet cut to a 3.500 x 1.178 inch rectangle and then rolled into a tubular form on a steel rod. The electrodes of the furnace held these pieces of molybdenum in the shape of a tube $\frac{3}{8}$ inch in outside diameter with only a slight overlap. It was found to be important to shape the molybdenum tubes on an oversized rod in order that the tubes would press against the inside walls of the electrodes with sufficient force to make good electrical contact while the tubes were operating at high temperatures. It was also necessary to leave some space between the ends of the tube and the shoulders of the electrodes in order to allow for thermal expansion and thus prevent buckling. Two concentric radiation shields, also made of molybdenum, were used and with these it was possible to reach temperatures in excess of 2000° C. without overloading the transformer.

Molybdenum tubes were also used as the heating elements for actual runs employing the zirconium oxide boats. These tubes were made as described above except that a $\frac{1}{4}$ inch hole was punched into the molybdenum sheet midway between the ends and 0.295 inch from one edge. The boat was

held in place with molybdenum spacers so that it was concentric with the tube and its hole coincided with that of the tube. A single radiation shield with a large rectangular gap in the top was used to reduce the radiation losses. With this arrangement temperatures over 1900° C. could be obtained with a current of about 230 amperes.

D. Temperature Regulator

The temperature control circuit designed by Davis was capable of holding the temperature in the furnace constant to better than 0.1 percent, but it had the following shortcomings:

1. The adjustments which had to be made on the variable resistors in order to bring the circuit into operation were extremely critical, and thus the proper settings were often difficult to locate.

2. The lowest temperature at which the control could operate was over 1200° C., yet temperatures as low as 1100° C. had to be controlled in runs on manganese.

3. The circuit could not always compensate for the large fluctuations in line voltage.

A few modifications overcame these deficiencies, however, and allowed the circuit to control the temperature within 0.1 percent over a range from 1100 to 2000° C.

The 931A photomultiplier was rewired so that there are 90 volts per dynode and the anode is at ground poten-

tial. The last stage of the photomultiplier current is fed through a fixed resistance and through two variable resistors for coarse and fine adjustments. The voltage drop across these resistors controls the operation of a miniature pentode whose plate current varies by roughly 10 percent for a change of 1 percent in the photomultiplier current. These amplified changes are then reflected into the primary circuit of the furnace transformer by means of three twin triodes which are connected in parallel with each other and with a low-voltage transformer in the furnace power circuit. A complete wiring diagram for the regulator is given in Figure 2.

For best operation the circuit requires a warm-up time of several hours. Otherwise, the initial fatiguing of the photomultiplier and the drop in battery voltages cause a gradual decrease in the feedback voltage. This change is sufficient to raise the temperature during a long run. During the warm-up period, light from the room is allowed to enter the photomultiplier housing through a hole which is just large enough to hold the photomultiplier current in its operating range. When the furnace has been brought to the temperature at which the run is to be made, the hole in the housing is covered as the iris diaphragm which controls the radiation from the furnace is opened. When the photomultiplier current reaches its operating range, a feedback voltage of from 2 to 9 volts is introduced into the furnace power circuit. This voltage is indicated

TEMPERATURE CONTROL CIRCUIT

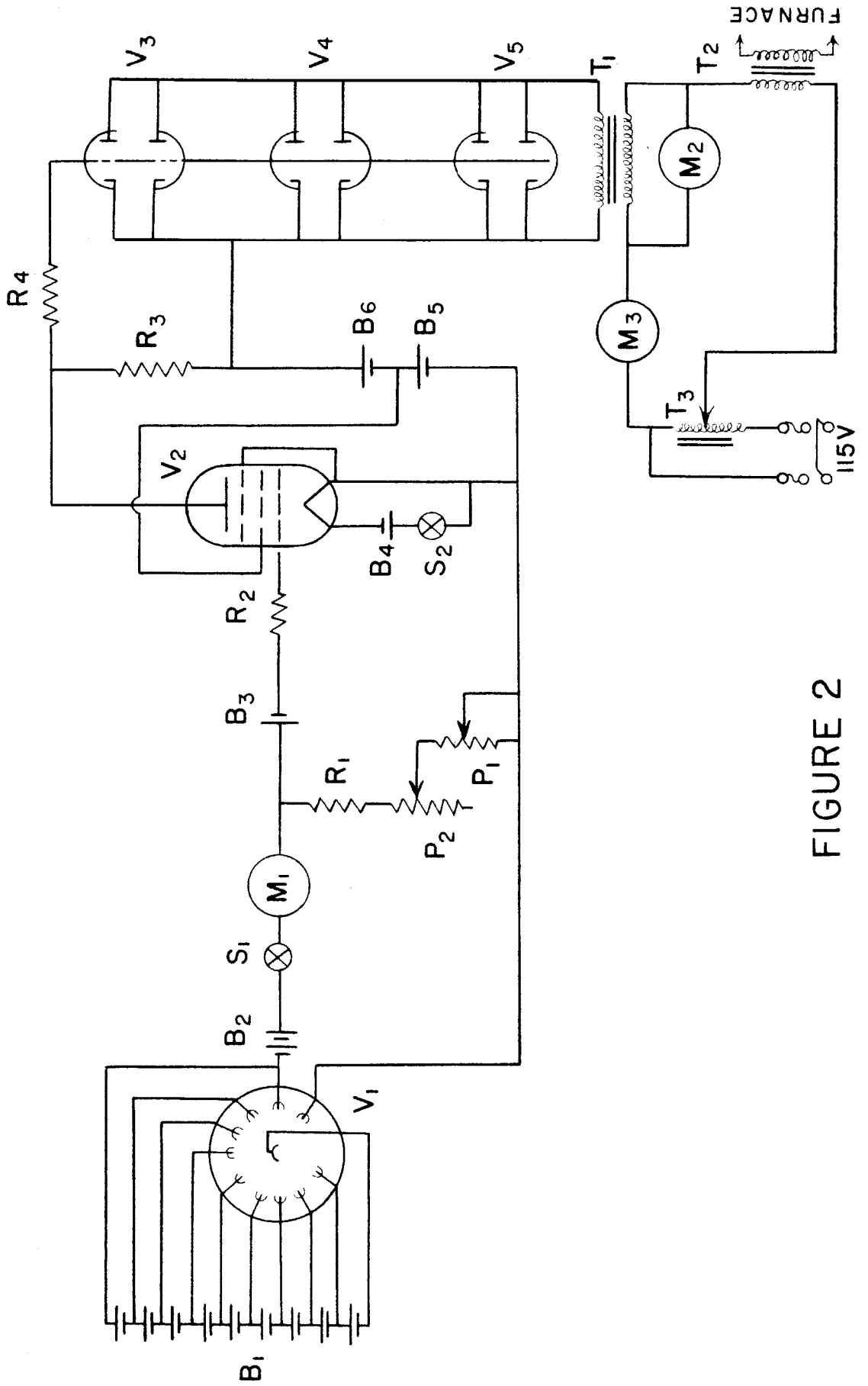


FIGURE 2

PARTS LIST

Batteries

- B₁ Battery Pack, 90 volt "B" batteries to supply dynodes
B₂ 2 90 volt "B" batteries in series
B₃ 67.5 volt "B" battery
B₄ 1.5 volt "A" battery
B₅ 90 volt "B" battery
B₆ 45 volt "B" battery

Tubes

- V₁ 931A photomultiplier
V₂ 3Q4 miniature pentode
V₃, V₄, V₅ 6AS 7 twin triodes

Resistors

- R₁ 1.0 megohms
R₂ 390 K ohms
R₃ 82 K ohms
R₄ 100 K ohms

Transformers

- T₁ 110 v - 5 v Kenyon
T₂ 110 v - 12 v 200 amp
Westinghouse
T₃ Variac 40 amp

Potentiometers

- P₁ 250 K ohms
P₂ 3 megohms

Meters

- M₁ 0 - 50 amp d.c.
M₂ 0 - 8 volts a.c.
M₃ 0 - 50 amp a.c.

Switches

- S₁, S₂ SPST

by the voltmeter, M_2 , and is set to fluctuate around the 5 volt mark by adjustment of the iris diaphragm.

The photomultiplier current at which the circuit regulates can be adjusted by means of the potentiometers P_1 and P_2 . The first of these gives a coarse adjustment and the second one a fine adjustment. For low temperatures (1100 to 1150° C.) these potentiometers should be turned to their lowest settings and the circuit will then regulate with a photomultiplier current of around 10 microamperes. For higher temperatures a photomultiplier current of 30 microamperes allows optimum operation of the circuit. Currents as high as 50 microamperes can be used, but it is better to use a filter in front of the iris diaphragm when very high temperatures are being controlled. This allows the diaphragm to be opened enough for good viewing of the furnace tube without causing the photomultiplier current to exceed the optimum value of 30 microamperes.

E. Microbalance Damper

The delicate quartz helix microbalance used to measure the density of atoms in the beam can be read with an accuracy corresponding to a few tenths of a microgram provided oscillations of the helix are at a minimum. However, large oscillations, introduced whenever the shutter between the balance pan and the boat is opened or closed, and smaller oscillations, introduced by sudden changes in the beam density or by particles sputtering from the boat,

can make the readings so crude as to be almost useless. In air, the oscillations are damped out immediately, but in a vacuum the larger oscillations will continue for several hours.

It was first thought that these oscillations might be damped out through eddy currents produced by a magnetic field in a vane attached to the helix, but a calculation showed this to be impractical. Because of the relatively slow motion of the helix (so-called large oscillations as viewed with the microscope actually have amplitudes amounting to only fractions of a millimeter), the vane needed with even a very strong magnetic field would have to have dimensions far in excess of that which the helix could support.

A suggestion by Dr. W. R. Smythe led to the following method of damping out all large oscillations. A small piece of iron wire cut 2 mm. in length and bent 180° at the middle was slipped over a loop at the bottom of the helix, and a coil of wire wound about the cylindrical glass housing of the balance was located just below the level of the iron piece. When a current is passed through the coil, the iron piece is pulled downward toward the center of the coil. Since the period of the fundamental mode of oscillation for the helix is about one second, the passage of current through the coil can be controlled manually in such a way that the force applied to the iron is opposite to the direction of motion during each half cycle and thus counter-

acts the oscillating movements. The coil consists of 30 turns of number 22 copper wire and is connected in series with a 3 volt battery, a variable resistor, and a key. By adjusting the variable resistor, enough current can be passed through the coil whenever the key is depressed to gently decelerate the oscillating balance. Generally only four or five such impulses are needed to bring the balance to a position of rest.

The only weakness in this damping method is that it cannot be used to damp out high frequency oscillations coming from other modes of vibration in the helix, since the period of these oscillations is too short to be followed manually. Fortunately, these oscillations have small amplitudes and if care is taken in the way the balance is used, they can be kept at a minimum. An electronic instrument could be devised to follow these rapid oscillations and feed a compensating current in opposite phase into the coil, but it is felt that the need for such a device does not justify the time required to design and build it.

F. Microbalance Pans

The pans on which the deposits from the beam are collected and weighed are made of 0.0008 inch aluminum foil cut with a stopper-cutting tool into 5/8 inch circular discs. These are placed in a specially made shaping-die which turns up the edge like a pie crust, thus giving the disc strength against curling. A short piece of 0.003 inch tungsten wire

is used to attach the pan to the quartz fiber of the micro-balance.

Originally, the suspension wire was attached to the pan with a speck of Duco cement, but it was discovered that the cement outgassed when the pan was exposed in a high vacuum to the hot furnace, and this introduced errors into the beam density measurements. Hence, the suspension was changed so that no glue is required. To accomplish this, the tungsten wire is passed through a tiny hole in the center of the pan. The lower end of the wire is given a circular bend which supports the pan in a horizontal position, and the upper end of the wire is bent into the shape of a small hook which slips into a loop at the end of the quartz fiber. With the aid of the shaping-die, a number of pans can be made in a short time, and the wire suspension can be used over and over again by merely straightening and rebending the hook.

G. Recorder Installation

In order to make an instantaneous measurement of the rate at which atoms are being deposited on the balance pan, a Brown Recorder was installed in the following way. First, a 10 K ohm precision Heliopot was coupled to the knob of the micrometer eyepiece used to measure fine displacements of the balance pan. A 1.5 volt battery was then connected in series with a 22 K ohm resistor, a switch, and the ends of the Heliopot coil. The voltage existing between the

end of the coil and the sliding contact is fed into the recorder so that each setting of the micrometer eyepiece corresponds to a position of the recorder pen. As the movement of the balance pan is followed manually by keeping the cross hair fixed on a point of the helix, the recorder produces a graph of balance pan position versus time. The slope of this graph can then be used to compute the rate of deposit, and changes in slope indicate changes in the deposit rate. Two turns on the eyepiece micrometer, corresponding to a deposit of 64 micrograms, produce full scale deflection on the recorder, but the eyepiece can be set back to zero at any time by moving the whole telescope on its micrometer screw.

H. Microphotometer

All of the equivalent width measurements reported here were obtained from tracings made on an electronic recording microphotometer located in Robinson Laboratory of the California Institute of Technology. This instrument uses a Leeds and Northrup Recorder to record the shape of the absorption line. A variety of magnification factors are available by changing the gear ratios which determine the motion of the plate carriage and the drive of the recorder paper. One such combination gives a magnification factor of 108 and this was used for all tracings. The recorder produces a tracing of the line on a strip of paper

$9\frac{1}{2}$ inches wide, so that the depth of a medium line can be measured to an accuracy of about 2 percent. All lines were traced twice, first in the direction of increasing wave length and then in the opposite direction, in order to detect errors which might be introduced by the microphotometer.

Focusing of this instrument presents no problem but alignment of the absorption lines with the slits of the microphotometer is not so simple since most of the lines are too weak to be seen in the magnified field. To aid in this adjustment, the emission spectrum of an iron arc was photographed at the bottom of some of the plates and these iron lines could then be easily aligned with the microphotometer slits. Generally a slit length slightly less than the width of the spectrum was used in order to minimize the effect of grain. The calibration plates were traced with the same microphotometer settings except for an increase in the drive speed of the plate.

IV. EXPERIMENTAL ANALYSIS AND TECHNIQUES

A. Scattered Light

Because scattered light in the spectrograph tends to fill in the absorption lines, resulting in f-value measurements that are too low, an intensive investigation was undertaken to determine the magnitude of this source of error. Though the presence of some scattered light was detectable even with the eye by looking at the grating in the ultra-violet region, early attempts to measure the amount of this light failed to reveal its true magnitude because of the high contrast and reciprocity law failure of the photographic plates used. Finally, with the aid of low contrast plates developed in a low contrast developer, it was discovered that the scattered light amounted to a surprising fraction of the dispersed light coming from the grating. The details of this measurement were as follows.

With a constant light source focused on the spectrograph slit, an exposure was made of sufficient duration to bring up a fairly dense image on a Kodak 33 plate in the 3250A region of the spectrum. A filter which cut off all light below 4300A was then placed over the slit and a second exposure of equal duration was made on the same plate. This plate together with a step slit calibration plate was then developed in D-23 developer for 5 minutes. The second image was dense enough to give a good micro-

photometer measurement which, when compared with a similar measurement on the first image, revealed an intensity ratio of 0.33 for the two exposures. Since the first exposure was made with dispersed light plus scattered light, this meant that at least 49 percent of the light reaching the plate in the 3250A region was scattered light of wave lengths greater than 3400A. Several checks of this kind were made and in each case the scattered light was found to contribute 30 to 50 percent of the exposure. Such measurements of course tell nothing about how much scattered light comes from the region below 3400A, and so the estimate given here must be taken as a lower limit on the percentage of scattered light.

It was obvious then that some means had to be found to eliminate this source of error. Dr. P. M. Routly proposed that this be accomplished by inserting a foreprism into the optical system. This prism and its monochromator action has already been described in Section III B. The effectiveness of the device is believed to be complete for two reasons. First, it is difficult to imagine how a significant amount of scattered light can arise from the narrow band of wave lengths admitted to the spectrograph and, second, all f-value measurements made since installing the foreprism have been greater than the preliminary measurements by a factor roughly equal to the estimated value of the total scattered light.

B. Beam Distribution

Another source of serious error could result from an atomic beam distribution which differed significantly from that assumed in the theory. It is not difficult to conceive of reasons why the beam distribution might be quite different from that of the theory since some of the assumptions made are not completely fulfilled. In the first place, the dimensions of the orifice in the boat far exceed that theoretically required to guarantee a Boltzmann velocity distribution inside the boat. Secondly, for some of the runs on copper, the molten metal, held by its own surface tension in the form of a ball, rested directly beneath the hole so that many of the atoms in the beam may have come directly from the metal surface. That these atoms take on a Boltzmann distribution is questionable. Thirdly, in a few cases where very strong absorption lines were sought, the vapor pressure in the boat may have been sufficient to cause a mass flow rather than an effusion of atoms. And finally, though the size of the hole is small compared with the dimensions of the beam, it does not actually constitute a point source and this may significantly affect the beam distribution. In regard to this last point, Heavens⁽¹⁶⁾ discusses the way in which collisions at the orifice due to short mean free paths may extend the effective area of the orifice, and if this should turn out to be a large effect, the beam distribution could cer-

tainly be affected. Another way in which the effective size of the atomic beam source could change is by penetration of the vapor through the walls of the boat. This phenomenon is known to be a problem in vapor pressure measurements, particularly with copper in graphite containers. Such possibilities as these certainly warranted a careful check on the actual beam distribution.

Davis recognized these possibilities and used an ingenious method employing a radioactive material to check experimentally the actual density distribution. Though his experimental results were in fairly good agreement with the theoretical distribution, it was felt that the test was not conclusive, particularly since it had not been carried out under a variety of conditions. Therefore, another method was devised for checking the distribution and this was carried out for several temperatures and for different sizes of the hole from which the beam emanates.

In this method the beam was allowed to form a deposit on a carefully cleaned glass plate located 6.15 cm. above the beam source. Immediately upon removal from the vacuum chamber, a microphotometer tracing of the thin metallic film formed on the glass was obtained. This tracing showed the variation in optical transmission of the film as a function of distance along the plate. However, it is well known that the absorption of light by a thin metallic film is not a linear function of the thickness and so this tracing

had to be calibrated in some way which would relate transmission of light to actual deposit thickness. This calibration was accomplished by placing a smaller glass plate in the furnace above the beam but this time allowing only a small area directly over the center of the beam to receive a deposit. A shutter between the source and the plate was used to control the time during which the deposit was made and a device for moving the plate between exposures was added to the apparatus. The plate was shifted by simply winding a cord onto a pulley inside the furnace container. This could be done in a matter of seconds without any disturbance to the vacuum. Thus, a series of deposits were made on the second glass plate with exposure times of 10, 15, 20, 30, 40, 60, 90, 120, and 180 seconds. Since the area of each deposit subtended the same small solid angle of the beam, the thicknesses of the films thus formed were proportional to the time of exposure, provided the deposit rate remained constant. To check the deposit rate, the 180 second exposure was immediately followed by three more exposures of 20, 30, and 60 seconds. These were then used as checks against earlier exposures to make sure that the deposit rate had not changed. This calibration plate was also measured on the microphotometer immediately upon removal from the vacuum chamber in exactly the same way as the first plate. Thus, changes in the films due to aging should not have affected the results.

Finally, from the microphotometer tracing of the cali-

bration plate a plot of the logarithm of the percent transmission of light as recorded by the microphotometer versus time of exposure was made for each deposit. A logarithmic plot was used because it gave a curve with a linear portion, very much like the characteristic curve of a photographic plate. From this curve points on the first tracing were reduced to values of the film thickness, in the arbitrary units of seconds, and these values were then plotted as functions of linear distance from the center along the plate.

Theoretically, the relation between deposit rate on a horizontal surface and linear distance from the center of the deposit is:

$$G(r) = G(0) \frac{b^4}{(b^2 + r)^2} \quad (13)$$

where

$G(0)$ is the deposit rate at the center of the horizontal surface directly above the furnace opening,

$G(r)$ is the deposit rate at the distance r measured along the horizontal surface from the center of the deposit, and

b is the vertical distance between the beam source and the horizontal surface.

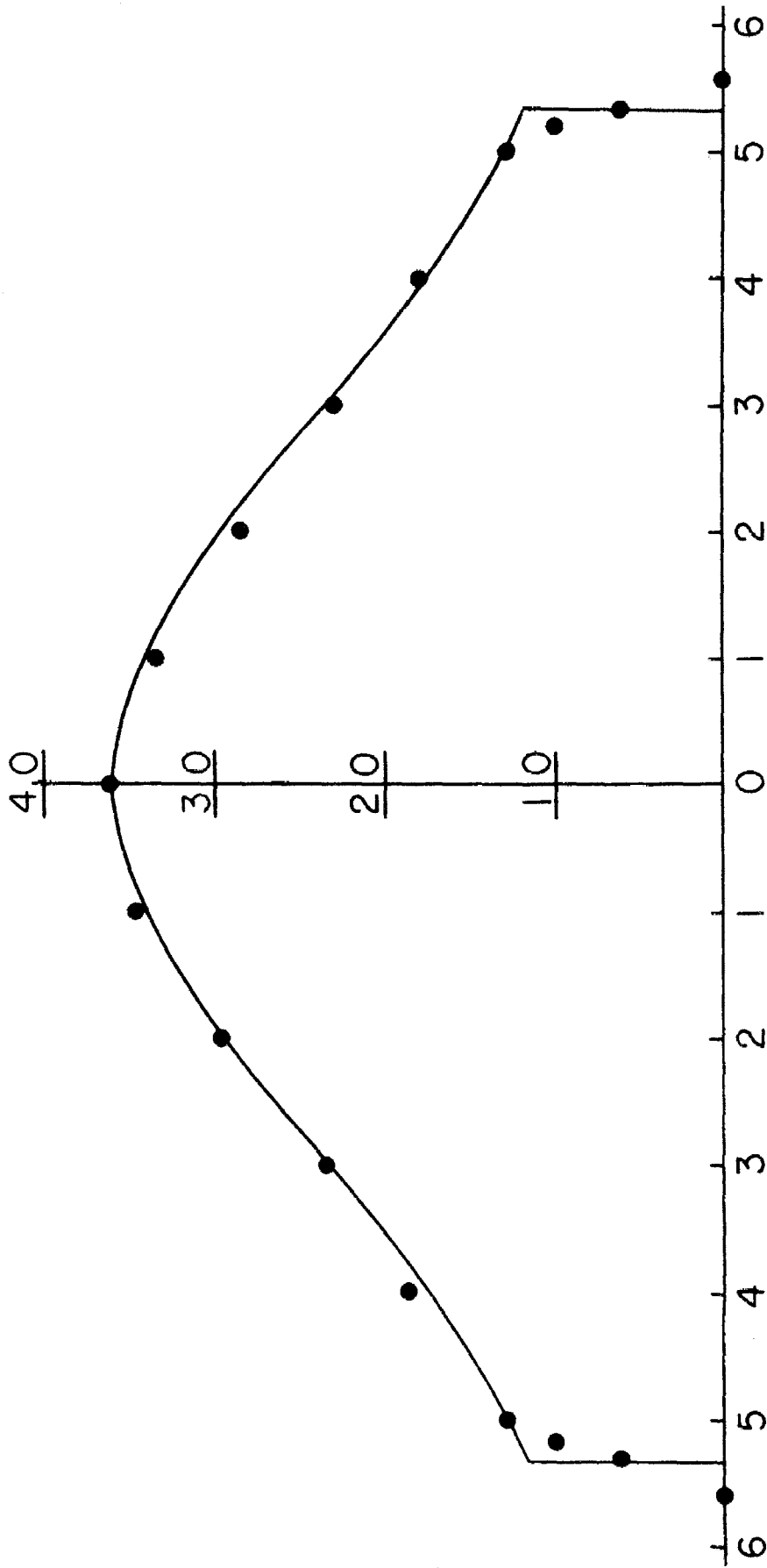
Taking the measured thickness of the deposit at the center

as $G(0)$, a theoretical plot of $G(\bar{r})$ versus \bar{r} can be graphed and compared with the experimental values for $G(\bar{r})$.

Figure 3 is a typical example of the graphs obtained from these tests. The solid curve in this figure represents the theoretical relation and the dots represent experimentally measured points. Beam density distribution checks were made under a variety of conditions and in each case a graph very similar to the one shown in Figure 3 was obtained.

The agreement seems to be remarkably close except for a few aspects which are easily accounted for. Because of the finite area of the source, the peak at the center of the experimental curve is slightly flattened. At the edges of the beam, the theoretical curve falls sharply to zero, while the experimental one falls off in a steep but not sharp tail. This too is caused by the finite area of the source, and the extent of the penumbra as measured from the experimental tracing agrees very closely in each case with that computed from the dimensions of the orifice and defining slot. Thus, the source does not behave as though its effective area were extended by collisions, nor does the beam distribution suggest that the effects of copper penetrating through the walls of the boat and tube are significant. To summarize, these checks indicate that the density distribution in the actual beam does not differ in any significant way from that assumed in the theory, and

ATOMIC BEAM DISTRIBUTION



DISTANCE FROM CENTER OF ATOMIC BEAM (Cm.)

FIGURE 3

therefore it can be concluded that only insignificant errors in absorption measurements will come from this source.

C. Reflection of Atoms

A third possible source of error can arise in the deposit rate measurements used to determine the actual concentration of atoms in the beam. It is assumed that all atoms which strike the balance pan stick there without any reflection, that is, that the accommodation coefficient is unity. A convincing test of this assumption under conditions of the experiment is needed.

The first attempt to detect any reflection of atoms which might occur made use of a method devised by Kopfermann and Wessel,⁽¹¹⁾ who also checked this source of error in their experiment. A deflector made of the same aluminum foil from which the balance pans are cut was placed at an angle above the hole through which a part of the beam normally comes to the balance pan. The orientation of this piece of foil was such that if atoms were reflected from it they would be deflected downward and to one side of the hole. The balance pan was located at the side toward which the reflected atoms were deflected and in such a way that the pan could not receive any of the upward moving atoms of the direct beam. If all atoms did not stick to the deflector, some should have been deposited on the top of the balance pan and detected by the effect of their weight on the balance. This test gave negative results;

that is, no reflected atoms were detected. However, this result was not entirely conclusive since not all deflected atoms could be expected to fall on the balance pan and quite a large number would have to deposit there for detection.

A more sensitive test was made by cutting a hole in a carefully cleaned piece of plate glass and placing this on the top plate of the furnace assembly so that its hole just coincided with that in the top plate. The glass was shielded completely from the direct beam and yet allowed a sample of the beam to pass through as before. Again, an aluminum deflector was placed in line with the hole in such a way that reflected atoms would be deflected to one side. On the top of the glass plate, two narrow strips of mica were laid with their long axes extending radially away from the edge of the hole. These strips protected small regions of the glass plate from exposure to reflected atoms and thus provided clean areas which could later be compared with exposed areas. After a heavy deposit had been allowed to fall on the deflector, the glass plate was removed from the apparatus, the mica strips were taken away, and the surface of the plate was traced with a microphotometer.

If a significant number of atoms had been reflected from the aluminum deflector, the microphotometer tracing should have revealed two effects. First, the areas protected by the mica strips should have transmitted more

light than the exposed areas when scanned by the micro-photometer, and second, the region of the plate toward which the deflector was turned should have shown more deposit than the region on the opposite side of the hole.

Very slight deposits were detected on these test plates except where the mica strips had lain, but these deposits were uniform over all parts of the plate, even over those regions farthest from the hole. On subsequent tests, smaller glass plates were placed at various locations inside the container. These showed the same uniform but faint coatings found on the test plate and so it was concluded that the deposits were due to vapors present throughout the apparatus but not due to atoms reflected from the aluminum. These tests were accepted as ample evidence that the accommodation coefficient is unity for the elements investigated.

D. Impulse Forces

There are two important features of the atomic beam experiment which enter directly into the theory used in the determination of absolute f -values. One is the density distribution of the atomic beam and the other is its velocity distribution. A check on the density distribution has already been described. A series of tests related to the velocity distribution will now be discussed.

The continuous transfer of momentum between the depositing atoms and the balance pan constitutes an upward

force which can be computed and also measured experimentally. The relation needed to compute this force has been given in Section II, equation 12. Experimentally, the force is given by the difference in microbalance readings taken just before and just after the shutter is opened and again just before and just after the shutter is closed. When the shutter is opened, oscillations of the helix are introduced, and these oscillations must be damped out before an accurate reading of the balance pan position can be made. Since a significant deposit is received by the pan during this time, the first impulse force measurement is not accurate unless a correction is made for this small deposit. When the shutter is closed, no further deposit is received by the balance pan and the impulse force can be measured directly with fair accuracy.

Table I gives the results of these measurements. In these data there are errors due to inaccuracies in the microbalance readings. Since these inaccuracies enter into the deposit rate values used to compute the force, they affect the calculated force determinations as well as the observed force measurements. Nevertheless, the data can be examined for systematic discrepancies.

In general, there is fairly good agreement between the observed and calculated forces. However, there are several possible sources of error which could cause significant differences between them, and it is worthwhile to consider these in some detail.

TABLE I

Impulse Force Measurements

(In Eyepiece Divisions)

	<u>T°K.</u>	<u>Calculated Force</u>	<u>Observed Force</u>		<u>T°K.</u>	<u>Calculated Force</u>	<u>Observed Force</u>
Cu	1618	6	6	Mn	1338	64	62
	1630	10	10		1350	73	72
	1631	12	14		1370	82	81
	1656	10	9		1382	88	87
	1675	10	9				
	1681	18	21	Fe	1962	131	129
	1722	38	46		2080	142	152
	1741	46	52		2100	257	339
	1748	21	23		2139	388	370
	1762	21	21		2203	598	474
	1774	25	24				
	1776	38	39	Cr	1667	8	6
	1783	23	22		1734	18	20
	1819	55	69		1735	19	19
	1833	140	164				
	1840	133	139				

1. The measured deposit rate may be in error due to reflection of atoms from the balance pan. If reflection occurs, the computed force will be too low since it is calculated from the measured deposit rate assuming that all atoms stick. Reflected atoms actually transfer added momentum to the pan but escape the deposit rate measurement.

The effect appears to be present in the data on impulse forces for copper, since there are a number of cases where the computed force is less than the observed force for this element. However, this effect was checked by an independent experiment (see Section IV C) and that investigation gave no indication of reflected atoms from the balance pan. Therefore, it can be assumed that the discrepancies are due to other effects.

2. The deposit rate may change due to variations in the surface of the evaporating metal or exhaustion of the metal sample. Then the force observed at one instant will not generally agree with the computed force calculated on the basis of an average deposit rate measured over the total time that the shutter is open.

It is quite possible that this effect causes many of the minor differences seen in the data on all four elements. Impulse force measurements made as the shutter was opened did not always agree well with measurements made as the shutter was closed. Most of this disagreement was due

to inaccuracies in the readings but some of it was caused by a changing deposit rate. In the absolute f -value measurements, data were discarded when this effect appeared to be present.

3. A significant fraction of the beam may be made up of molecules rather than single atoms. The effect of molecules in the beam is to give an observed force which is smaller than that computed for a monatomic beam, as the following derivation shows. Let X be the fraction of the deposit rate, G , which is monatomic, the remainder, $1 - X$, being diatomic. Then from equation 12 the force, F , due to the momentum transfer of these two types of particles is

$$F = F_1 + F_2 = \frac{3\sqrt{\pi}}{4} \sqrt{\frac{2RT}{M}} XG + \frac{3\sqrt{\pi}}{4} \sqrt{\frac{2RT}{M}} (1 - X)G$$
$$F = \left(\frac{3\sqrt{\pi}}{4} \sqrt{\frac{2RT}{M}} G \right) \cdot \left(X + \frac{1 - X}{\sqrt{2}} \right) \quad (14)$$

The first factor in parentheses in the final expression for F is exactly the force calculated under the assumption that the total deposit is monatomic, and the second factor in parentheses has a value that is less than or equal to unity. Thus, for a given deposit rate, the effect of molecules in the beam is to decrease the observed force.

This effect is especially important in the case of Cu I where a diatomic molecule is known to exist. However, since there is no systematic indication of the observed force being less than the calculated force in the case of copper, this test for the presence of Cu_2 molecules was taken to be negative. No molecules of the other three elements investigated here are known to exist, and there is no indication of a molecular effect in the impulse force data for these elements.

4. The temperature inside the boat, as measured with the optical pyrometer, may differ from the effective temperature related to the root-mean-square speed of atoms escaping through the hole of the boat. This effect could arise from the use of a relatively large hole as an orifice in the boat or by allowing atoms to escape directly into the beam from the free surface of the molten metal. It was shown in Section IV B that these deviations from an ideal beam source do not significantly affect the beam density distribution, but this does not guarantee that the velocity distribution is unaffected.

Since only the square root of the absolute temperature enters into the calculations of an impulse force, the temperature read with the pyrometer would have to be in error by quite a large factor in order to cause a significant difference between the calculated and observed forces.

Thus, this test is not a sensitive one for errors in temperature. Fortunately, however, the absolute f-value calculations also involve only the square root of the absolute temperature, so small errors in the temperature are not significant anyway.

The four effects just discussed are the major sources of error which could cause the calculated and observed forces to differ. Analysis of the data has shown that, although the forces did not always agree exactly, no serious sources of systematic error in the experiment were indicated.

E. Deposit Rate Measurements

The quartz helix microbalance used in determining the beam density extends 1.000 cm. for a change in weight of 986 micrograms. The position of the balance is read with the aid of a microscope mounted on a micrometer which can be read to 0.001 cm. and estimated to 0.0001 cm. The microscope itself possesses a micrometer eyepiece and in most cases the extensions of the helix were measured with this eyepiece rather than with the microscope micrometer, since the former can be adjusted and read more easily. One division on the micrometer eyepiece corresponds to 0.000230 cm. and thus a change in weight of a few tenths of a microgram could be detected.

Several different techniques were applied to the deposit rate measurements.

1. With the shutter closed, the balance pan position was read with the micrometer eyepiece. The shutter was then opened, allowing the pan to collect a deposit of atoms

from the beam for a measured length of time. At the end of this time, the shutter was closed and a second balance pan position was read. The difference between these two position readings was divided by the time the shutter was open to give the deposit rate in eyepiece divisions per second. The spring constant and conversion factors given above were used to convert the deposit rate to micrograms per second.

Several difficulties were involved in this technique. After the shutter had been opened and closed several times, rapid, uncontrollable oscillations of the helix were often observed. These oscillations reduced the accuracy with which extensions of the helix could be measured so that uncertainties of 10 divisions were not uncommon. Thus, total extensions of at least 100 divisions had to be observed in order to make the readings accurate to 10 percent. Since the deposit rates were of the order of 1 division per second, this meant that deposit times of more than a minute had to be used. Such deposit times were more than twice the exposure times needed for photographing the absorption lines. It was extremely difficult to obtain a series of deposit rate measurements at one temperature by this technique, because a constant atomic beam could generally not be maintained for the total time required.

2. In order to shorten the time needed for a series of deposit rate measurements, the technique of making these

measurements with the shutter continuously open was tried. The balance pan then experienced no great changes in the impulse force, and oscillations were almost nil. Consequently, determinations of the balance pan position could be made to an accuracy of about 2 divisions. When timed with a stop watch the deposit rate measurements could be made over short intervals of time and a rapid series of such determinations could be obtained while the atomic beam remained more or less constant.

This technique also had disadvantages. Whenever the beam density varied, the impulse force as well as the actual deposit rate changed. For iron, where high temperatures and large deposit rates were used, the impulse force corresponded to several hundred eyepiece divisions. Since this force was directly proportional to the deposit rate, a change of 10 percent in the latter caused the balance to fall by some 20 divisions. If such a change took place gradually over a period of time, say one minute, it produced an apparent change in the deposit rate which may have been as much as 30 percent of the actual deposit rate.

Since the impulse force and the deposit weight are oppositely directed, the apparent change in the deposit rate due to a changing impulse force is opposite to the actual deposit rate change. It is even conceivable that the changing impulse force could exactly compensate for a changing deposit rate in such a way that the open-shutter observations would indicate a constant deposit rate. However, the

exact conditions needed to cause this are very unlikely to occur, and thus changes in the actual atomic beam density were generally indicated by the observed deposit rate.

In some runs, particularly on iron, the individual determinations of the deposit rate for one temperature did not agree very well, indicating that the atomic beam density had indeed changed. In order to detect changes in the beam density as they occurred, an instantaneous measurement of the deposit rate was needed. The installation of the Brown Recorder (See Section III G) permitted such an instantaneous measurement and introduced the following technique for deposit rate determinations.

3. With the shutter closed a reading of the microbalance position is made visually with the micrometer eyepiece. The shutter is then opened and two stop watches are started. As soon as large oscillations of the helix have been damped out, one of the stop watches is stopped and the new position of the microbalance is read with the micrometer eyepiece. Then while a series of photographic exposures is being made, the position of the balance is continually tracked with the eyepiece cross hair, allowing the recorder to trace a graph of balance position versus time. The slope of the recorder trace indicates the deposit rate at each instant. Marks are made on the recorder tracing to indicate the time intervals during which each photographic exposure is made. At the end of the last photographic exposure, the position of the balance

is read with the micrometer eyepiece, and immediately the shutter is closed as the second stop watch is stopped. Finally, the position of the balance is read with the shutter closed.

From the four visual position readings of the balance the following information can be derived. The difference between the first and last reading divided by the time during which the shutter was open, as indicated on the second stop watch, gives the average deposit rate. This can then be compared with the slope of the recorder tracing. If the recorder tracing shows no significant changes in slope and agrees in general with the average rate, then it is assumed that the beam density has remained constant. The difference between the first two visual readings plus the deposit rate multiplied by the time needed to damp out oscillations, as indicated by the first stop watch, gives the impulse force at the beginning of the run; the difference between the last two visual readings gives the impulse force at the end of the run. These impulse force measurements can be compared with each other as a further check on the constancy of the beam density and can also be checked with the impulse force calculated on the basis of the observed temperature and deposit rate. Finally, an attempt can be made to correlate any changes in slope that do show up on the recorder graph with differences in the corresponding equivalent widths of the observed spectral lines.

It is felt that this technique, though somewhat complicated, allows a maximum of information to be derived from each run and provides the best basis for analysis of the f-value data.

F. Calibration of Optical Pyrometer

The optical pyrometer used for all temperature measurements was calibrated against a similar instrument recently standardized at the Leeds and Northrup factory. This calibration included a correction for the light losses in the windows of the furnace through which the boat is viewed. The following derivation shows how the calibration can be accomplished by determining for each temperature scale of the pyrometer a constant which relates the observed and true temperatures.

An optical pyrometer matches the intensity of light radiated from a standard source, such as a lamp filament, with the intensity of light radiated from the object whose temperature is desired. The wave length of the light admitted to the pyrometer in this matching process is limited to only a short interval of the visible spectrum, generally in the red region. The temperature scale of the pyrometer is based upon Wien's Law for the distribution of energy in the spectrum of a black body. By an application of Wien's Law, the scale can be corrected for temperature measurements on non-black bodies and for readings made through slightly absorbing materials. To derive the

correction formula, we begin with the following form for Wien's Law:

$$J_{\lambda} = c_1 \lambda^{-5} e^{-c_2/\lambda\theta} \quad (15)$$

where

J_{λ} is the intensity at the wave length λ ,

λ is the wave length measured in microns,

c_1 is a constant which, as will be seen below, drops out of the final expression,

c_2 is a constant = $\frac{hc}{k} = 14,350$ microns-degrees, and

θ is the absolute temperature of the black body.

The intensity of radiation J_{λ}' , from a non-black body of temperature T and emissivity E_{λ} is given by

$$J_{\lambda}' = c_1 E_{\lambda} \lambda^{-5} e^{-c_2/T\lambda} = c_1 \lambda^{-5} e^{-c_2/S_{\lambda}\lambda} \quad (16)$$

where S_{λ} is the equivalent black body temperature at wave length λ of the emitter. It is this temperature which is indicated by the optical pyrometer when it views the non-black body. From the last equation

$$\frac{1}{T} - \frac{1}{S_{\lambda}} = \frac{\lambda \log_{10} E_{\lambda}}{6232} \quad (17)$$

Thus, knowing λ and E_{λ} , it is always possible to compute the true temperature, T , from the observed temperature, S_{λ} . The optical pyrometer used here employs a red glass filter which transmits light at $\lambda 0.65$ microns. The value of E_{λ} depends upon the wave length, λ , as well as the

nature and state of the emitting material. For example, the value of E_λ at $\lambda 0.65$ microns for iron in the molten state is 0.37.⁽¹⁷⁾

When an emitter is sighted with the optical pyrometer through windows, prisms, lenses, etc. where absorption takes place, the observed temperature, S_λ , is less than the true temperature, T , in much the same way as when a non-black body is sighted. Thus, the relation between S_λ and T under these conditions is given by

$$\frac{1}{T} - \frac{1}{S_\lambda} = A \quad (18)$$

where A is a constant for most practical purposes.

In the determination of the constant A , the optical elements and apertures of the furnace should be located in exactly the same relative positions as those existing during the temperature measurements. Then, if one of the windows or holes through which the light must pass cuts into the light cone, the resulting decrease in intensity and corresponding apparent reduction in temperature will be corrected for. This effect may actually exist in the present experiment since slightly different corrections were obtained before its significance was recognized.

During the calibration process, a tungsten filament lamp controlled by a Variac was used in place of the furnace tube and boat. The filament of this lamp could be seen through the optical system of the furnace and also could be viewed directly with the factory calibrated pyrometer.

Thus, a series of readings for each scale was taken with the two pyrometers, and by substitution in equation 18 the following mean values of the constant A were obtained:

<u>Pyrometer Scale</u>	<u>A</u>
Low	-0.000014 ($^{\circ}\text{K}$) ⁻¹
High	-0.000017 ($^{\circ}\text{K}$) ⁻¹

The extra-high scale (above 1750^o C.) was used in only a few instances and then the temperatures were only slightly above those which could be read on the high scale. By taking readings on a tungsten filament lamp in the region of overlap for the high and extra-high scales, it was found that 10^o C. should be added to temperatures read on the lower part of the extra-high scale. This correction was applied to temperatures read on the extra-high scale.

The temperature measurements used for absolute f-value calculations were made by sighting into the cavity in the boat where the radiation field closely resembles that of a black body. Observed temperatures checked well with the known melting points of the elements as observed in the bottom of the boat during the change of state. However, in one or two cases, the molten metal came to the hole of the boat in the form of a ball sufficiently large to completely block the opening. Then it was no longer possible to sight into the cavity and temperature readings had to be made on the surface of the molten metal. In order to

reduce these temperature readings to true absolute temperatures, equation 17 was used. Generally, this condition could be avoided by increasing the temperature very slowly in the melting point region, and only one run was carried out with the hole completely blocked. In all other cases, very little or none of the sample was visible through the hole of the boat and a good black body temperature reading could be obtained.

G. Continuum

The image of the light source as it is focused on the spectrograph slit has a length along the slit of about 3 mm. This refers of course to the width of the spectrum focused there when the foreprism is used. Due to the astigmatism of the spectrograph, this short illumination of the slit gives a spectrum at the plate holder which is about 5 mm. wide. This spectrum is not equally intense across its full width but has edges which are less intense than the center. Normally, there is a region of uniform intensity a few millimeters wide along the center of the spectrum, and an adjustable slot just beneath the plate holder is set to admit only this part of the beam. However, with the complicated optical system needed for this experiment, even the central region of the spectrum is not uniform but is striated with narrow lines of various intensities.

If accurate measurements of equivalent widths are to be made, these striations in the continuum cannot be toler-

ated, since the microphotometer tracing will include several of them and thus cannot be correctly calibrated. A great amount of time was spent in seeking to locate and eliminate the source of this difficulty. Finally, it became apparent that a great variety of defects ranging from flaws in the quartz water jacket of the mercury lamp to aberrations in the lenses were contributing to the problem, and to eliminate all of these simultaneously was impossible. Thus, a device was incorporated into the optical system which tends to smooth out the illumination along the slit during the exposure. This device consists essentially of a movable lens holder; its design has already been described in Section III B. The essential feature of the mechanism is that it allows the lens to be moved back and forth in a direction parallel to the slit and thus track the image of the light source along the slit without changing either the focus or the wave length range passed by the slit-foreprism combination. Though the lens holder is designed to give the image a full displacement of 3 cm. along the slit, a movement of the image of only 2 or 3 mm. is generally sufficient to smear out the major striations.

H. Equivalent Width Measurements

As far as random errors are concerned, the weakest link in the determination of absolute f -values by the method described here probably lies in the measurement of

the equivalent width of the absorption lines. Flaws in the photographic emulsions, plate grain, inaccuracies in the plate calibration curves, microphotometer fluctuations, and asymmetric line profiles are some of the factors which contribute to the uncertainty of the equivalent width measurements. For this reason a number of exposures (generally six or seven) were made at each temperature setting. The random scatter in a set of equivalent width measurements made under constant conditions was sometimes as high as 30 percent, but the average measurement gave an f -value consistent with those obtained on other runs.

The method used in reducing the microphotometer tracings was essentially the same as that used by Hill.⁽¹⁵⁾ However, only the profiles of the weakest lines were treated as simple triangles. For strong lines and asymmetric lines the intensity profiles were divided into horizontal strips and the equivalent widths were obtained by summing the areas of the strips.

In exposing the step slit calibration plate for each run, extreme care was exercised in stabilizing the tungsten ribbon filament lamp at the desired intensity. The electrically timed shutter guaranteed uniform exposure times and simultaneous development with the absorption line plates insured equal development. Still there existed the possibility of error due to non-uniform illumination of the larger steps by the enlarged image of the ribbon filament. To investigate this a series of test calibration curves

were made using different lamp intensities and the same exposure time. Because of the different lamp intensities, the linear portions of these curves were defined by different sets of steps. Though there were slight differences at the extreme ends of the characteristic curves, the linear portions agreed very well in all cases. Therefore, it is believed that the equivalent width measurements contain only random errors and are as accurate as can be made photographically.

V. RESULTS AND CONCLUSIONS

In the following sections, the results of absolute f -value measurements obtained in the present experiment for resonance lines of Cu I, Mn I, Fe I, and Cr I are recorded and discussed. One line of each element has been chosen for detailed investigation. The data for these lines are given in tables at the end of each section. These data have been obtained by averaging all values of the deposit rate, G , and all values of the equivalent width, W , measured under one set of conditions, and a weight has been assigned to each set of measurements. The weights are based on a scale of 1 to 10 and depend upon the number of independent equivalent width and deposit rate measurements, the degree to which the atomic beam seemed to have remained constant, and the quality of the photographic exposures. This last factor is especially dependent upon the part of the calibration curve of the photographic plate used in reducing the equivalent width measurements, since the linear part of this curve yields results which are much more reliable than the knees. The mean value of all individual determinations for a line has been taken as the absolute f -value of the line. Absolute f -values for other lines have then been obtained by making measurements relative to the line of each element which was chosen for detailed investigation.

The final data for one line of each element are represented graphically by plotting the experimental values of $\log W/\Delta\lambda_D$ versus $\log G/QT$, and each of these experimental plots is fitted to the theoretical curve of growth ($\log W/\Delta\lambda_D$ versus $\log C$) by the method outlined in Section II. The theoretical curve is shown by the solid line in these graphs and dots represent the experimental values.

In the last section a summary of all absolute f -values is given with a comparison of corresponding absolute f -values obtained by other investigators.

A. Copper

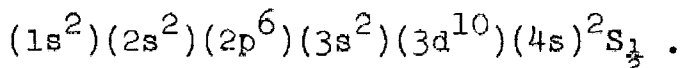
1. Background

As mentioned in the introduction, it was felt that the atomic beam method for measuring absolute f -values needed thorough checking before it could be depended upon to give reliable values for elements of astronomical interest. For making the required checks, an element with some rather special properties is needed. First, it is desirable to investigate an element that can easily be contained while in the liquid state. Second, the temperature at which the element produces an effective atomic beam should lie in a range which does not require excessive power for the furnace design and which can easily be measured with the optical pyrometer. Third, the element should have some strong lines in the visual or near ultra-violet region.

Finally, it would be very desirable to investigate an element for which something is already known of the absolute f-values.

Copper appeared to fulfill these requirements. It gives a usable beam in the temperature range of 1200 to 1700° C.; it evaporates uniformly from a graphite boat with no sign of combining with the carbon; it has very strong lines at λ 3247 and 3274 which are accessible to the apparatus with its quartz optical system; and the absolute f-values of these lines have been measured by King and Stockbarger⁽³⁾ using the absorption tube method. Thus, while copper is not of particular astronomical interest, it has been extensively investigated here in order to check the experimental technique and the accuracy attainable.

The electron configuration of the neutral copper atom in the ground state is



Because there is only one (4s) electron outside a closed shell, the low lying states of copper have approximately hydrogen-like wave functions. These known wave functions allow a theoretical estimate of the absolute f-values to be made for the resonance lines of copper with some validity. (See Bates and Damgaard.⁽⁸⁾)

King and Stockbarger's experimental measurements, originally based on the vapor pressure data of Harteck,⁽¹⁸⁾ gave absolute f-values of 0.62 and 0.32 for the lines λ 3247

and $\lambda 3274$ respectively. However, if more recently obtained vapor pressure data by Hersh⁽¹⁹⁾ and by Hultgren⁽²⁰⁾ are applied to the measurements of King and Stockbarger, absolute f -values of 0.52 and 0.27 are obtained for the lines $\lambda 3247$ and $\lambda 3274$ respectively. The method outlined in Section II for taking hyperfine structure into account must be used in reducing all data on the copper resonance lines since these lines do exhibit hyperfine structure. As shown by King,⁽³⁾ only two components of intensity ratio 5:3 need be considered, and thus each value of $W/\Delta\lambda_D$ has been divided into two parts with this ratio of intensities in determining the corresponding value of C .

2. Copper Molecule

In the course of investigating a discrepancy between f -values obtained in the present experiment and those obtained by King and Stockbarger, it was learned that a diatomic copper molecule exists in vapors of this element. This molecule was discovered by Kleman and Lindkvist⁽²¹⁾ who identified the Cu_2 bands obtained in emission with a King furnace. With the help of Mr. K. H. Olsen, the author photographed the Cu_2 bands in absorption using the large King furnace located at the Mt. Wilson Laboratory on Santa Barbara Street in Pasadena. The bands lying in the $\lambda 4000$ to $\lambda 5000$ region were brought out very strongly in a helium atmosphere of 40 cm. pressure at a temperature of 1950°C ., but they were not at all visible at tempera-

tures below 1500°C. The presence in the same spectra of very broad resonance lines of atomic copper as well as other strong atomic lines showed that the density of copper atoms in the vapor was very high, but it was impossible to estimate from the strengths of the bands and atomic lines anything about the ratio of molecules to atoms.

In a letter from the University of Chicago, Dr. Mark G. Inghram states that a mass spectrograph study of Cu_2^+ ions in the vapor from a Knudsen cell loaded with copper has been carried out by one of his students, Mr. Paul Schissel. Unpublished data on these experiments indicate that the ratio of Cu_2^{63+} ions to Cu_1^{63+} ions in a vapor at 1300 to 1400°C. is only about 0.002 to 0.003. If this ratio is valid for the atomic beams used in the present experiment, then such a small fraction of molecules would not affect the absolute f-value results.

There still remains, however, the possibility that more molecules are present in an atomic beam, which is formed almost directly from an evaporating surface, than are present in the Knudsen cell used by Inghram or in the absorption tube used by King and Stockbarger where equilibrium conditions exist. In order to approach more closely the equilibrium conditions in an absorption tube, a special boat was machined from graphite. This boat was somewhat longer than that normally used and it contained small molybdenum partitions located approximately 3/16 of an inch from each end. These partitions closed off each end of

the boat except for a small opening at the top. Copper samples were placed in the ends behind the partitions and the ends were then sealed with graphite plugs as usual. In this boat it was impossible for the molten copper to flow into the central region of the cavity and to effuse atoms directly into the beam. Also, since the orifice in this special boat was smaller than that usually used, it was felt that a better equilibrium between molecules and atoms, due to multiple collisions, would be established before atoms found their way out into the beam.

A number of runs were made with this special boat, but both impulse force and absolute f -value measurements were the same as those obtained with the ordinary boats. Though this cannot be considered a conclusive test as to the presence of small numbers of Cu_2 molecules in the atomic beam, the negative results indicate that Cu_2 molecules do not exist in the atomic beam in numbers sufficient to account for the discrepancy between results obtained here and those obtained with the absorption tube. On the basis of Dr. Inghram's work, it can be concluded that, at the temperatures used in any of the present absolute f -value measurements, copper molecules probably do not contribute sufficiently to the atomic beam to cause significant errors in the results.

3. Data

Table II gives the pertinent data for the resonance line, $\lambda 3247$, of Cu I. By varying the temperature over the range 1200 to 1700^o C., and by using triple as well as single traversals of the light beam, it was possible to experimentally define the curve of growth for this line of copper from the linear region to a part which is well up on the knee of the curve. This is brought out clearly by the plot shown in Figure 4. The fact that the experimental points in this plot can be fitted with a horizontal shift of the theoretical curve of growth (the vertical position having been fixed by $\sin \gamma$) is taken as one of the best indications that this experiment does give results which vary with experimental conditions as the theory predicts. Further, the good agreement between single beam and triple beam points in the region where these results overlap indicates that the triple beam theory is correct.

The theoretical curve of growth relation has not been tabulated for values of C greater than 10, but an approximate equation for the curve of growth when C is large has been used to extend the theoretical curve shown in Figure 4. The extended portion is indicated by the dashed curve. The experimental points which lie in this extended region are useful in providing a graphical comparison with the theory for strong lines but are not individually very reliable for absolute f -value determinations because of the small slope

of the curve of growth in this region. Hence, the quantity C and the absolute f -values for these points have not been included in the data given in Table II or in the mean value of the absolute f -value for the line.

Though the slit-foreprism combination was set to pass only a short region of the spectrum centered at $\lambda 3247$, the "continuum" provided by this pass sometimes extended above $\lambda 3280$. In such cases f -value measurements could be made on the other resonance line of copper at $\lambda 3274$. The f -value for this weaker line, $\lambda 3274$, relative to that of the stronger line, $\lambda 3247$, was found to be 0.53. This relative value agrees quite well with the relative strengths of these two lines as measured by King and Stockbarger.⁽³⁾

The final results of all absolute f -value measurements for the two lines of Cu I are as follows:

Transition	λ	f	Average Deviation
$4^2S - 4^2P_{\frac{1}{2}}^0 - 3/2$	3247.54	0.310	± 0.026
$\frac{1}{2} - \frac{1}{2}$	3273.96	0.164	± 0.037

TABLE II.

DATA FOR Cu I, $\lambda_{3247.54}$

	T° K	G μgm/sec	G/QI	W x 10 ³ Å	W/Δλ _D	W/Δλ' _D	C	f	Wt.
(1)	1453	0.0264	1.86	3.61	0.538	0.854	0.531	0.285	5
(2)	1535	0.0628	4.16	7.66	1.11	1.76	1.24	0.299	4
(3)	1535	0.0530	3.51	6.85	0.993	1.58	1.08	0.308	4
(4)	1564	0.0381	2.47	5.47	0.785	1.25	0.815	0.330	3
(5)	1564	0.0330	2.15	5.63	0.808	1.28	0.843	0.393	2
(6)	1564	0.0335	2.17	5.01	0.718	1.14	0.736	0.339	4
(7)	1595	0.0575	3.66	5.38	0.766	1.22	0.793	0.217	3
(8)	1612	0.0239	4.01	8.60	1.22	1.93	1.40	0.349	9
(9)	1617	0.0964	6.06	10.2	1.44	2.29	1.76	0.291	2
(10)	1617	0.0680	4.27	7.30	1.03	1.64	1.13	0.266	2
(11)	1617	0.0526	3.30	6.79	0.960	1.52	1.04	0.315	2
(12)	1633	0.0306	2.11	4.79	0.674	1.07	0.684	0.324	2
(13)	1654	0.114	7.02	10.5	1.47	2.33	1.80	0.256	1
(14)	1687	0.0536	3.88	7.87	1.09	1.73	1.21	0.312	2
(15)	1689	0.0183	1.10	2.22	0.307	0.487	0.290	0.263	8
(16)	1703	0.107	6.38	11.0	1.51	2.40	1.88	0.296	3
(17)	1703	0.0745	4.44	8.69	1.19	1.90	1.37	0.307	6
(18)	1712	0.0237	1.41	3.64	0.499	0.792	0.489	0.348	10
(19)	1717	0.0948	5.61	10.2	1.40	2.22	1.69	0.301	1
(20)	1722	0.0312	1.84	3.91	0.535	0.849	0.528	0.287	7
(21)	1722	0.0837	5.48	10.3	1.40	2.23	1.69	0.309	2
(22)	1722	0.0967	6.33	11.2	1.53	2.43	1.91	0.302	4
(23)	1733	0.0201	1.18	3.18	0.434	0.688	0.420	0.357	3

TABLE II (Cont.)

	T° K	G μgm/sec	G/QT	W x 10 ³ Å	W/Δλ _D	W/Δλ' _D	C	f	Wt.
(24)	1733	0.0879	6.20	11.3	1.55	2.45	1.94	0.313	2
(25)	1733	0.0876	6.18	11.5	1.58	2.50	2.00	0.324	2
(26)	1775	0.226	12.9	16.1	2.17	3.45	3.40	0.263	5
(27)	1775	0.213	32.4	24.7	3.33	5.29	12.0	0.371	5
(28)	1775	0.238	36.3	26.6	3.59	5.69			5
(29)	1775	0.220	33.5	26.7	3.60	5.72			1
(30)	1780	0.444	62.1	25.3	3.40	5.40			3
(31)	1785	0.0582	3.31	7.12	0.956	1.52	1.03	0.312	4
(32)	1819	0.736	101	27.7	3.69	5.86			3
(33)	1822	0.327	20.2	20.3	2.70	4.28	5.55	0.302	6
(34)	1828	0.453	67.0	31.5	4.18	6.63			2
(35)	1828	0.494	73.1	28.1	3.73	5.92			2
(36)	1838	0.202	11.2	16.8	2.22	3.53	3.55	0.318	1
(37)	1838	0.270	14.9	17.8	2.36	3.74	4.02	0.269	1
(38)	1892	1.13	149	30.8	4.02	6.38			1
(39)	1979	0.853	43.8	25.1	3.21	5.09			1

Weighted Mean f = 0.310

Cu I $\lambda 3247$

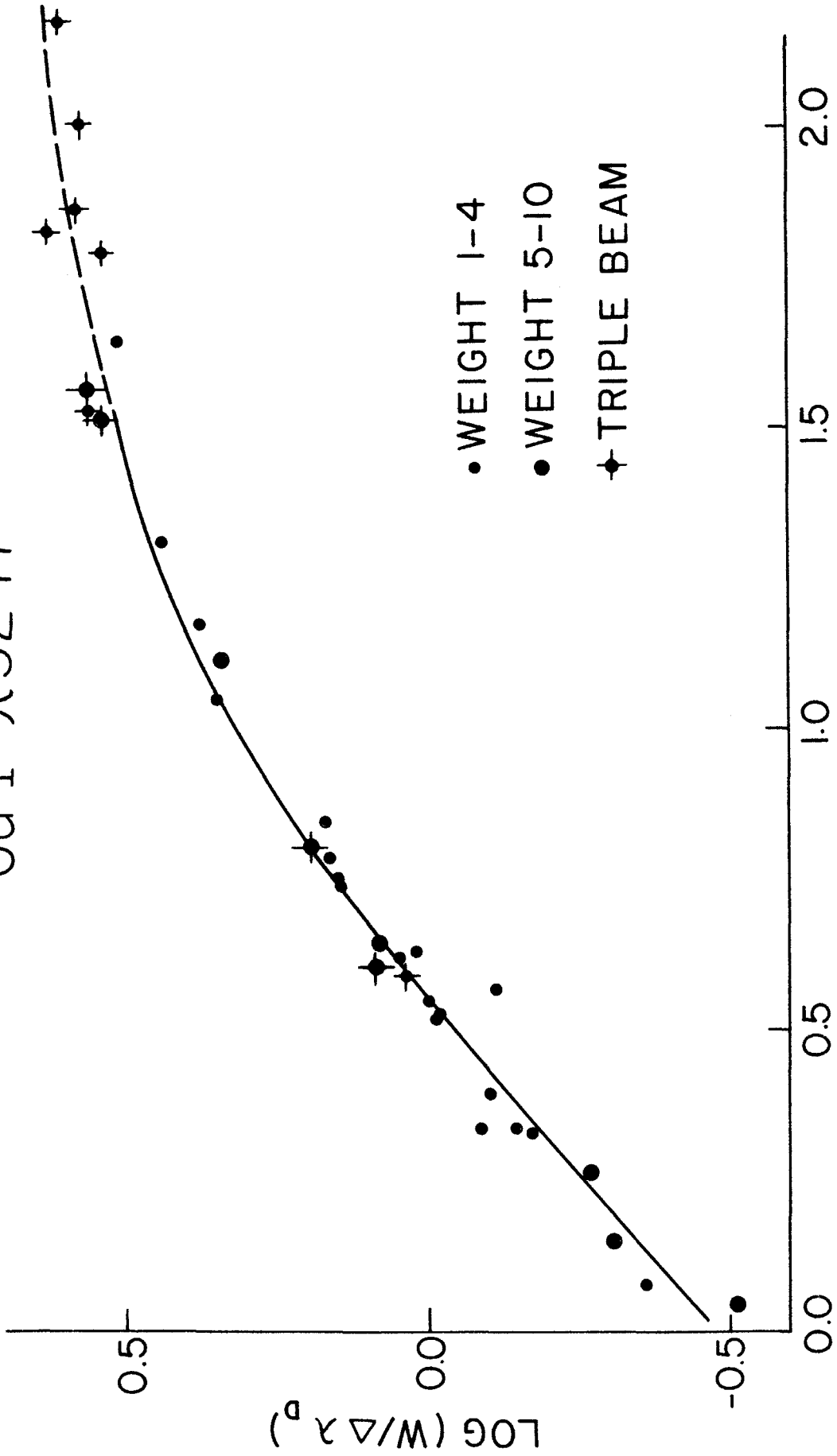


FIGURE 4

B. Manganese

1. Background

Very little work has been done on absolute f-values for manganese, and no experimental determinations of relative f-values have been made for this element. The only lines which arise from the ground state and appear in the visible or near ultra-violet region belong to the triplet ($a^6S-z^6P^o$), $\lambda\lambda$ 4031, 4033, and 4034. These are the only lines that can be investigated by the atomic beam method. This triplet is of some astrophysical importance since it is observed in solar and stellar spectra and thus can be used for abundance determinations.

The absolute f-values of these lines were measured by Huldt and Lagerqvist⁽⁷⁾ using the emission spectra of a manganese salt sprayed into a flame. The values which they reported for this triplet are:

Transition	λ	f
$a^6S - z^6P^o_{5/2-7/2}$	4030.75	0.062
$5/2-5/2$	4033.07	0.046
$5/2-3/2$	4034.49	0.031

These determinations agree surprisingly well with the values obtained in the present experiment, considering that the method employed by Huldt and Lagerqvist is questionable and yields values for Cr I which are apparently too low by a factor of 100.

2. Hyperfine Structure

It was pointed out in Section II that hyperfine structure may contribute to the broadening of a line in such a way that the line will not follow the usual curve of growth. Specifically, if the components of the hyperfine structure are separated by distances greater than their doppler widths, then each component should be treated as a separate line, each following its own curve of growth. If the hyperfine structure is not completely resolved by the spectrograph, the measured equivalent width of the unresolved line is the sum of the equivalent widths of the components of the line.

Manganese has a nuclear spin of $5/2$ and a magnetic moment of 3.4 ; thus it exhibits large hyperfine splitting. At first it was thought that this splitting would be sufficient to cause the observed manganese lines, which are unresolved blends of the hyperfine structure components, to follow a linear curve of growth over the range of beam densities used in these experiments. However, a closer investigation of the hyperfine structure makes this assumption dubious.

The strongest line, $\lambda 4031$, of the triplet under consideration here arises from the $a^6S_{5/2} - z^6P_{7/2}^o$ transition. Hyperfine splitting of both the lower and upper states gives rise to 15 hyperfine lines. However, because the splitting of the lower state is considerably less than that

of the upper state, these 15 lines fall into 6 major components. Using the tables of White,⁽²²⁾ these components are found to have relative intensities of 100 : 72.5 : 50.4 : 33.0 : 19.8 : 10.3, and they are spread out over a wave length interval of 0.050 Angstroms as shown in Figure 5. The theoretical magnitude of the splitting has been verified experimentally by White and Ritschl⁽²³⁾ and their results also indicate that the relative intensities are correct.

In the atomic beam experiment, the doppler width of a weak absorption line at half-intensity is given by

$$2 \sqrt{\ln 2} \Delta \lambda_D \sin \gamma = 2 \frac{\lambda_0}{c} \sqrt{\frac{2RT}{M} \ln 2} \sin \gamma$$

where $\sin \gamma = 0.63$. Thus, at an absolute temperature of 1350° K., the width of each component in the manganese line should be about 0.009 Angstroms. When this width is applied to each hyperfine component, as shown in Figure 5, the profiles of the components are found to overlap to a considerable extent. None of this structure is resolved by the spectrograph, of course, but this analysis indicates that the hyperfine-structure separations are not sufficiently larger than the doppler widths of the components to allow each component to contribute independently to the line. Thus, in the determination of the quantity C for the line, the experimentally measured equivalent widths cannot simply be split into parts corresponding to the inten-

HYPERFINE STRUCTURE OF MnI $\lambda 4031$

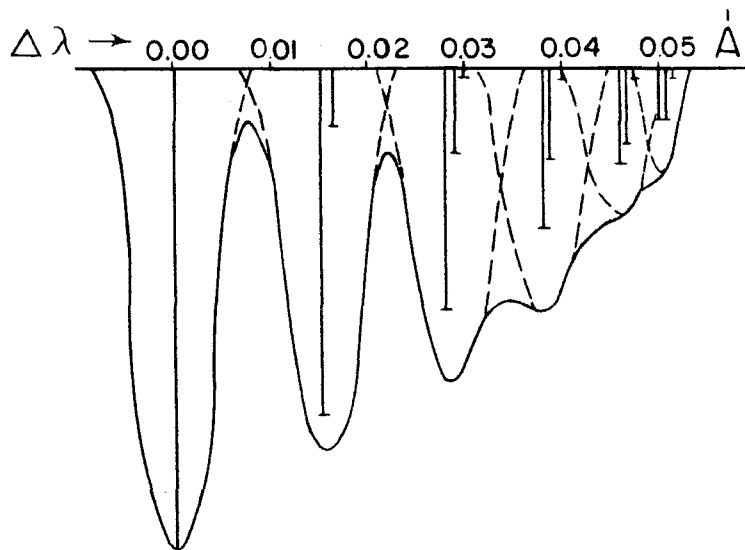
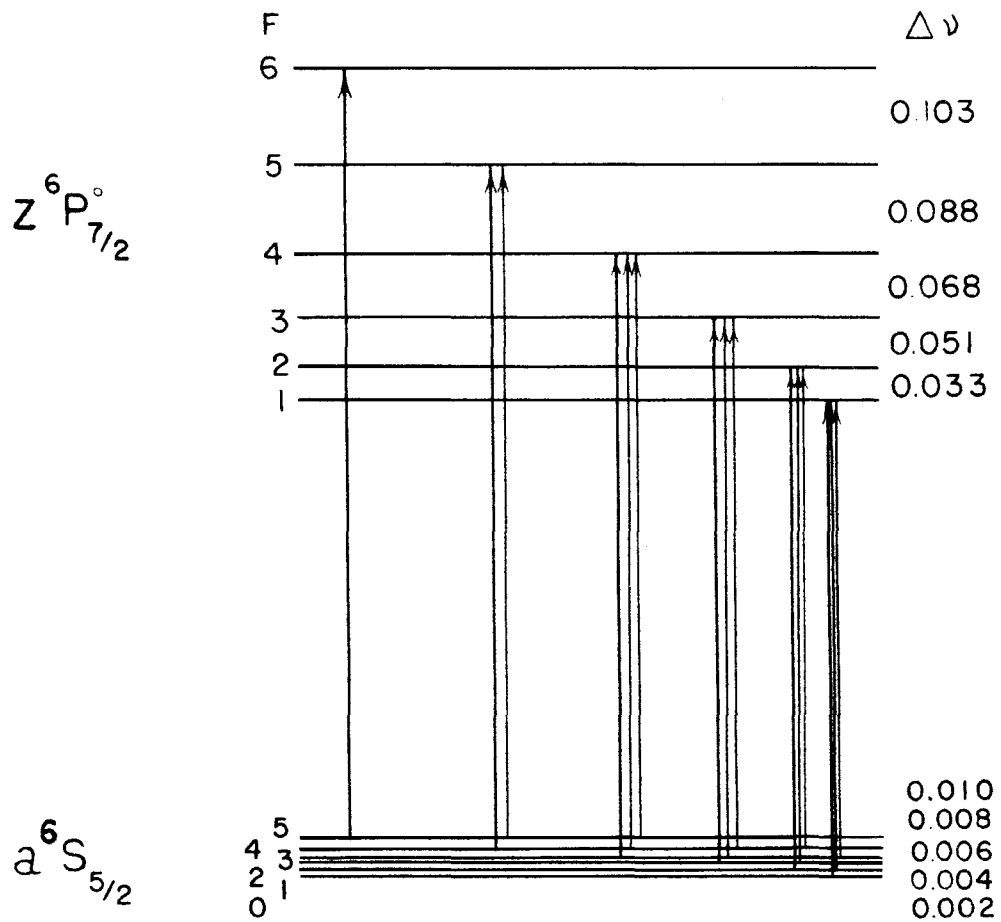


FIGURE 5

sities of the various hyperfine structure components.

The analysis above is verified qualitatively by the experimental results. When the equivalent width measurements are plotted to form a curve of growth, they cannot be fitted with a theoretical curve based on the complete splitting scheme. Though there is considerable scatter in the data, Figure 6 shows quite clearly that the curve defined by the experimental points is not the linear part of a curve of growth with its characteristic 45° slope.

The solid curve in Figure 6 is the theoretical, almost linear curve calculated on the basis of complete separation of the major components of the hyperfine structure. The dashed curve represents the curve of growth calculated with no splitting, which would apply if the hyperfine-structure separations were much less than the doppler widths of the components. Since the experimental points lie between these two curves, it is strongly suggested that the components do overlap as the theoretical consideration indicates.

This means that the line as photographed with the spectrograph has been broadened in a way which cannot be completely analyzed. However, it can still be safely assumed that when the lines are very weak they follow a nearly linear curve of growth, and therefore, these lines can be used in the absolute f-value determinations.

3. Data

Table III gives the averaged measurements made on the strongest line of Mn I, $\lambda 4031$, and Figure 6 is a plot of these data. A value for C and an absolute f-value have been calculated only for measurements made when the line was very weak, that is, for values of $\log G/QT$ less than 1.2. Since almost the same result is obtained for any scheme of splitting assumed in determining C for the very weak lines, they are evidently near enough to the linear part of the curve of growth to yield reliable f-values regardless of the exact character of the hyperfine structure. To obtain the results given in Table III, the values of $W/\Delta\lambda'_0$ were divided in the ratio 5:4:3, since this ratio corresponds to the relative intensities of the main hyperfine-structure components.

Most of the measurements were made on the strongest line, $\lambda 4031$, but some measurements of the f-values of the other two lines of the triplet relative to that of $\lambda 4031$ were made. The final results of all absolute f-value measurements for the three resonance lines of Mn I are as follows:

Transition	λ	f	Average Deviation
$a^6S - z^6P^o_{5/2-7/2}$	4030.75	0.0611	± 0.0052
$5/2-5/2$	4033.07	0.0343	± 0.0029
$5/2-3/2$	4034.49	0.0221	± 0.0019

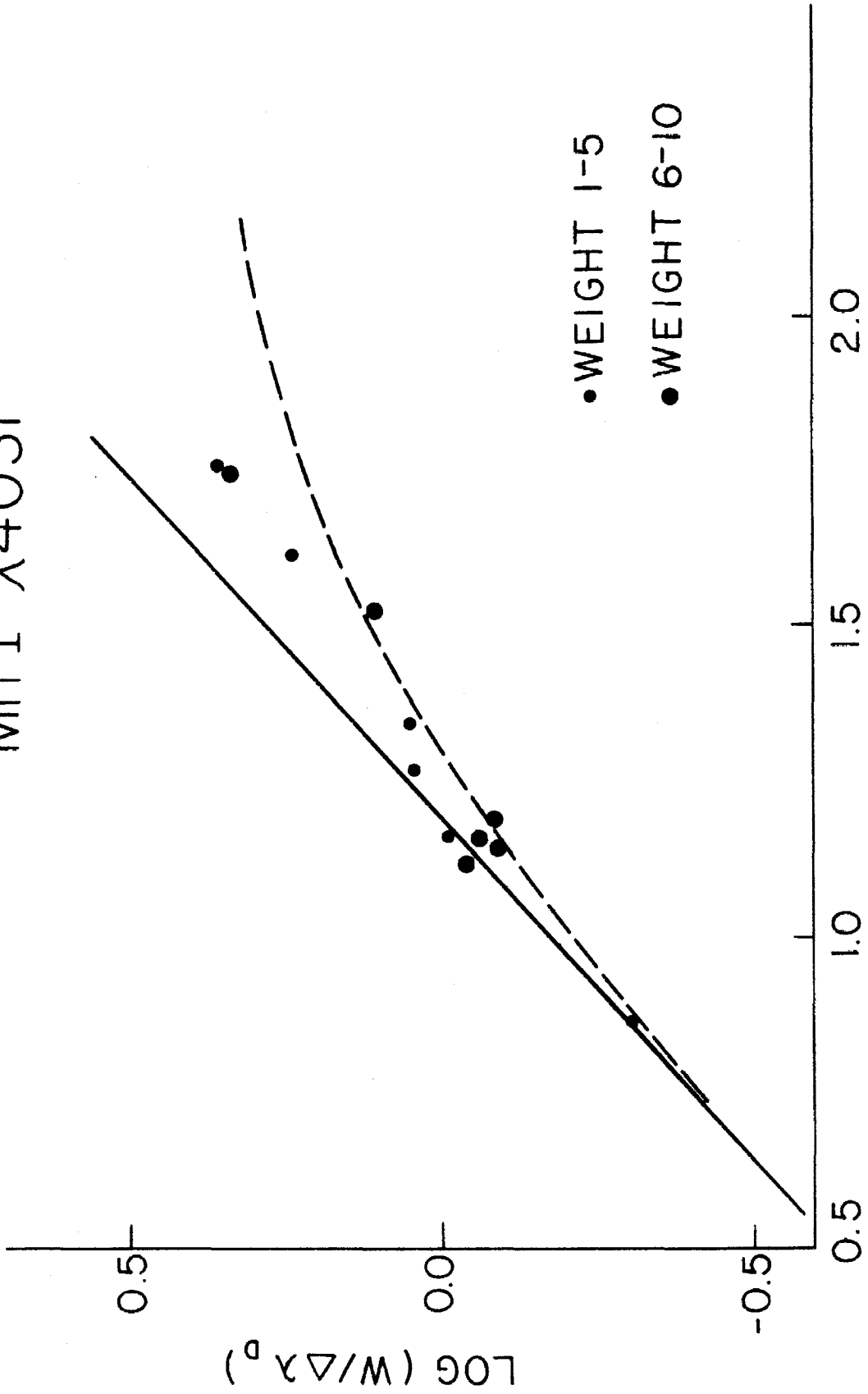
TABLE III

DATA FOR Mn I, λ 4030.75

	T° K	G $\mu\text{gm}/\text{sec}$	G/QT	W x 10 ³ Å	W/ $\Delta\lambda_0$	W/ $\Delta\lambda'_0$	C	f	Wt.
(1)	1309	0.0686	7.28	4.20	0.496	0.787	0.470	0.0646	6
(2)	1321	0.135	13.9	6.98	0.821	1.30	0.810	0.0582	6
(3)	1331	0.141	14.4	8.39	0.982	1.56	0.990	0.0687	3
(4)	1334	0.141	14.4	7.38	0.862	1.37	0.856	0.0594	7
(5)	1342	0.149	15.4	7.15	0.833	1.32	0.823	0.0534	10
(6)	1352	0.132	13.2	7.82	0.911	1.45	0.910	0.0691	8
(7)	1357	0.216	22.1	9.53	1.11	1.75			3
(8)	1368	0.189	18.6	9.53	1.10	1.75			4
(9)	1371	0.224	55.6	18.7	2.16	3.43			10
(10)	1373	0.332	33.5	11.0	1.27	2.10			6
(11)	1384	0.410	41.0	15.0	1.72	2.74			4

Weighted mean f = 0.0611

Mn I $\lambda 4031$



LOG (G/QT)
FIGURE 6

C. Iron

1. Background

Throughout the universe iron has an anomalous abundance relative to other elements of similar mass; in fact, the abundance of Fe^{56} is larger than the sum of the abundances of all other nuclear species with mass numbers greater than 40. Thus, it is of great astrophysical interest, and accurate determinations of its abundance in the sun and stars from spectrographic observations are important. In the past there has been considerable uncertainty in the exact astronomical abundance of iron because of disagreements between experimental absolute f -value determinations. It now appears, however, that these experimental results are converging toward a well-defined absolute f -value so that astronomical iron abundance measurements in the future should not suffer from uncertainties in this important factor.

Relative f -values for a large number of the Fe I lines, arising from the lower levels of the Fe atom, have been measured by King and King^(1,2) and by Carter.⁽²⁴⁾ King⁽⁴⁾ has also used the absorption tube method to make absolute f -value measurements on twelve lines from the ground state of Fe I. In his paper,⁽⁴⁾ King reported a value of 0.013 for the absolute f -value of the strongest line, $\lambda 3720$. This value was based on the vapor pressure data of Marshall, Dornte, and Norton,⁽²⁵⁾ but recently Edwards, Johnston,

and Ditmars⁽²⁶⁾ have published vapor pressure data which differs considerably from the earlier measurements. On the basis of the newer data, King's absolute f -value for the line $\lambda 3720$ is raised to 0.033. Using all existing data Hultgren⁽²⁰⁾ is now evaluating the thermodynamic properties of many elements and alloys including iron. On the basis of vapor pressure data given in this work, a third absolute f -value, 0.022, for the line $\lambda 3720$ of Fe I can be evaluated from King's measurements. These revisions clearly show the difficulties and uncertainties involved in vapor pressure measurements at the present time.

Kopfermann and Wessel,⁽¹¹⁾ using an atomic beam method, reported in 1951 an absolute f -value of 0.043 for the line $\lambda 3720$. This value is more than three times King's first value, but it is in closer agreement with King's revised values. Evenso, it is larger by some 30 percent than the highest value obtained from King's measurements. Kopfermann and Wessel also made measurements on the line $\lambda 3737$ and reported a value of 1.03 for the ratio of f_{3720}/f_{3737} . This is in good agreement with the relative intensities of these two lines as reported by King in his absolute determination.

With the atomic beam apparatus used here, it was possible to bring out a number of lines in the $\lambda 3700$ - $\lambda 3900$ region arising from the sublevels of the a^5D ground state of Fe I. Because of the narrow wave length pass needed to eliminate scattered light, however, only one or two of

these lines could be studied from one exposure. Since the relative strengths of these lines are well established, the absolute f-value investigation reported here was concentrated on the strongest line, $\lambda 3720$. Actually, the line $\lambda 3737$ fell in the usable region of continuum on many of the plates, but its observed intensity was always lower than that of $\lambda 3720$ by a factor of almost 2 because of the Boltzmann distribution of atoms over the sub-levels of the ground state. Thus, it was often too weak for accurate measurement. The few measurements which were made on the line $\lambda 3737$ yielded an f-value relative to that of $\lambda 3720$ which was in agreement with the relative f-values given above.

2. Boats and Tubes

As mentioned in Section III C, iron combines with the material of the boat to such an extent that the maintenance of a constant beam was extremely difficult. Boats made of zirconium oxide heated in molybdenum furnace tubes finally proved to be the most successful means for holding the iron samples. These were used for five of the nine runs for which data is given here. The first four runs employed graphite boats lined with tantalum carbide and heated in graphite tubes. Though the presence of graphite did not allow a constant beam to be maintained for any length of time and thus made some measurements

invalid, no systematic differences were observed in the results obtained with the two kinds of boats.

3. Data

Table IV gives the data for the line $\lambda 3720$ of Fe I, and Figure 7 shows a plot of $\log W/\Delta\lambda_0$ versus $\log G/QT$ taken from these data. The scatter in these data is considerably more than for copper because of the uncertainties involved in the measurement of weak lines and because of the difficulties in maintaining a constant atomic beam. Due to the Boltzmann distribution of atoms over sub-levels of the complex ground state of Fe I, only about half of the atoms in the beam are in the lowest sub-level of the ground state from which the line $\lambda 3720$ is absorbed. Because of this and the small f -value of the line, it was not possible to obtain strong lines well up on the knee of the curve of growth. Nevertheless, the experimental points shown in Figure 7 define a curve which, when fitted with the theoretical curve, yields an absolute f -value in good agreement with the absolute value obtained by averaging individual measurements. This average value is

<u>Transition</u>	<u>λ</u>	<u>f</u>	<u>Average Deviation</u>
$a^5D - z^5F_{4-5}^0$	3719.93	0.0316	± 0.0038

TABLE IV
DATA FOR Fe I, $\lambda 3719.93$

	T° K	G $\mu\text{gm}/\text{sec}$	G/QT	W x 10 ³ Å	W/ $\Delta\lambda_D$	W/ $\Delta\lambda'_D$	c	f	Wt.
(1)	1950	0.130	20.7	4.75	0.503	0.798	0.540	0.0261	6
(2)	1966	0.129	20.4	4.39	0.463	0.734	0.488	0.0239	4
(3)	1983	0.0683	10.7	4.15	0.436	0.691	0.455	0.0426	8
(4)	1985	0.112	6.92	2.08	0.219	0.347	0.211	0.0305	5
(5)	2003	0.0749	11.5	3.29	0.344	0.546	0.347	0.0302	6
(6)	2010	0.0481	7.37	2.65	0.276	0.438	0.271	0.0368	6
(7)	2020	0.0592	9.11	3.22	0.335	0.531	0.336	0.0369	7
(8)	2040	0.147	8.83	2.60	0.269	0.426	0.263	0.0298	5
(9)	2055	0.171	26.1	7.20	0.742	1.177	0.885	0.0339	5
(10)	2070	0.219	13.0	3.32	0.341	0.541	0.343	0.0264	3
(11)	2075	0.162	23.8	6.24	0.640	1.014	0.728	0.0306	8
(12)	2080	0.185	27.8	7.27	0.745	1.181	0.890	0.0320	7
(13)	2080	0.171	25.6	6.56	0.673	1.068	0.778	0.0304	7
(14)	2183	0.322	45.4	9.61	0.961	1.523	1.29	0.0284	3
(15)	2085	0.274	40.4	9.96	1.021	1.619	1.42	0.0351	6
(16)	2098	0.251	37.4	8.54	0.871	1.381	1.110	0.0297	10
(17)	2100	0.229	33.3	6.95	0.708	1.122	0.830	0.0249	6

Weighted mean f = 0.0316

Fe I $\lambda 3720$

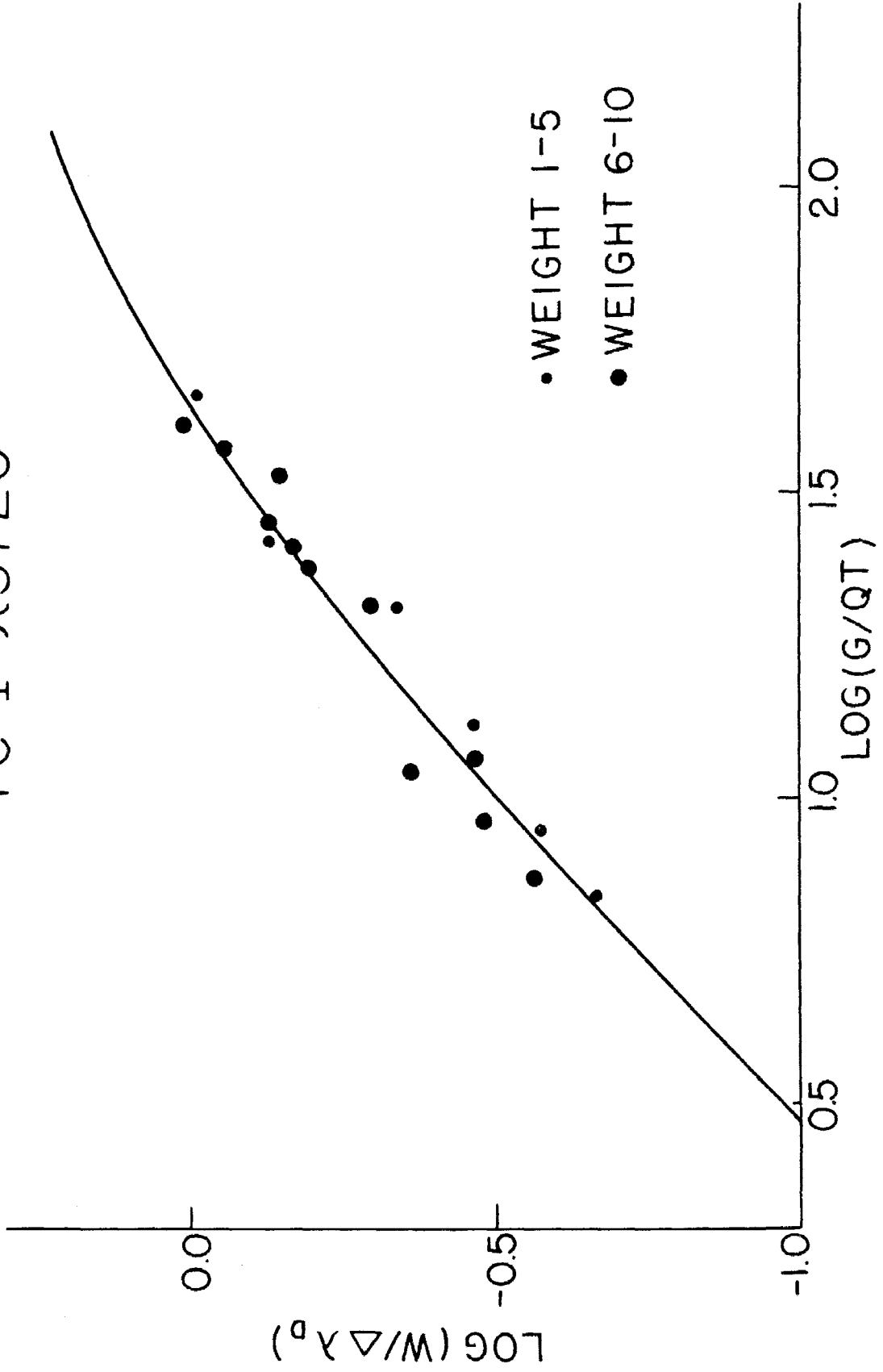


FIGURE 7

D. Chromium

1. Background

Chromium is of astrophysical interest since its lines are prominent in the spectra of the sun's atmosphere and its cosmic abundance is one of the highest of the iron group elements. An accurate determination of the cosmic abundance of chromium is important in defining the iron peak of the abundance curve. For this reason a careful determination of absolute f-values for lines of this element is of considerable value.

In the past there have been several investigations of absolute f-values for the Cr I resonance lines. Estabrook^(5,6) used the absorption tube method to determine absolute f-values for the lines λ 4290, 4275, and 4254. The values reported in his first paper⁽⁵⁾ were revised on the basis of improved vapor pressure data. These revised values as reported in Estabrook's second paper⁽⁶⁾ are as follows:

<u>Transition</u>	<u>λ</u>	<u>f</u>
$a^7S - z^7P_{3-2}^o$	4289.72	0.047
3-3	4274.80	0.067
3-4	4254.35	0.084

Huldt and Lagerqvist,⁽⁷⁾ using the method of spraying a solution of a chromium salt into a flame and making measurements of emission line intensities, reported for these

same lines absolute f-values which are smaller than those of Estabrook by a factor of about 100. Because of the extreme uncertainties in the concentration of chromium atoms in the experiment of Huldt and Lagerqvist, the results are likely to be unreliable.

Hill⁽¹⁵⁾ has made relative f-value measurements on 430 lines of Cr I including all of the resonance lines, $\lambda\lambda$ 4290, 4275, 4254; 3605, 3593, 3578. Thus, the results obtained here for the resonance lines can be used to put Hill's relative measurements on an absolute scale.

2. Boats

Chromium is different from the other elements so far investigated in that it has an appreciable vapor pressure at temperatures somewhat below its melting point (1615° C.) and can produce an effective atomic beam while still in the solid state. When the chromium sample is contained in a graphite boat there is sometimes a tendency for it to sputter, but it behaves very nicely in a graphite boat lined with tantalum carbide so long as the temperature is below the melting point. As the melting point is exceeded, the beam density increases for a brief time but then decreases to a very low value. This decrease takes place when either a graphite boat or a graphite boat lined with tantalum carbide is used and is apparently due to the formation of chromium carbide. In the case of the boat lined with tantalum carbide, the molten chromium quickly works its

way into deep pockets in the graphite. It also tends to flow out of the boat at the orifice, coating the lip of the liner and the edge of the graphite around the opening. Fortunately, the strongest chromium lines appear at temperatures below the melting point and since none of these difficulties is experienced so long as the chromium sample remains in the solid state, most of the runs reported here were made at temperatures below the melting point. Ceramic boats may successfully hold chromium in the molten state, but since they are difficult to make and since effective atomic beams could be obtained without them, they were not used.

3. Data

Table V gives the data for the resonance line $\lambda 4254$ of Cr I and Figure 8 shows a plot of $\log W/\Delta\lambda_0$ versus $\log G/QT$ taken from these data. Three of the 15 sets of data reported here were obtained when a graphite boat was used to hold the chromium sample and the remaining twelve sets of data were obtained with a graphite boat lined with tantalum carbide. In three cases the melting point of chromium was exceeded. In all other cases the chromium sample was in the solid state during evaporation.

The solid curve shown in Figure 8 is the theoretical curve of growth shifted horizontally to fit the experimental points. As in the case of iron, the scatter in

the experimental points is quite large, but from the 15 sets of data obtained, a fairly reliable mean absolute f-value for the line $\lambda 4254$ can be determined.

Equivalent widths of two other lines of Cr I, $\lambda 4275$ and $\lambda 4290$, could also be measured on most of the plates and from these measurements relative f-values for the triplet could be determined. Since the relative f-value calculations do not involve the atomic beam concentration measurements, they show less scatter than do the absolute f-value calculations. Relative f-values measured here for the three lines $\lambda 4290$, $\lambda 4275$, and $\lambda 4254$ are 0.589, 0.784, and 1.00 respectively. These relative values agree quite well with the values 0.567, 0.783, and 1.00 reported by Hill⁽¹⁵⁾ and 0.56, 0.79, and 1.00 reported by Estabrook.⁽⁵⁾

By taking the average of the absolute f-values given in Table V for the resonance line $\lambda 4254$ and then using the relative measurements obtained for the whole triplet, the following absolute f-values are obtained:

Transition	λ	f	Average Deviation
$a^7S - z^7P_{3-2}^o$	4289.72	0.0324	± 0.0041
3-3	4274.80	0.0431	± 0.0055
3-4	4254.35	0.0550	± 0.0064

From these results the factor by which Hill's⁽¹⁵⁾ relative f-values are to be multiplied to obtain absolute f-values is 3.9×10^{-4} .

TABLE V
DATA FOR Cr I, λ 4254.35

	T° K	G $\mu\text{gm}/\text{sec}$	G/QT	W x 10 ³ Å	W/ $\Delta\lambda_D$	W/ $\Delta\lambda'_D$	C	f	Wt.
(1)	1667	0.0212	4.53	2.30	0.546	0.348	0.211	0.0466	4
(2)	1667	0.0201	4.29	2.70	0.642	0.409	0.252	0.0589	5
(3)	1701	0.0343	7.18	3.17	0.747	0.476	0.297	0.0413	5
(4)	1704	0.0307	6.41	3.62	0.850	0.542	0.344	0.0537	6
(5)	1734	0.0408	8.36	4.79	1.02	0.713	0.472	0.0565	4
(6)	1734	0.0408	8.83	4.66	1.09	0.692	0.456	0.0516	4
(7)	1734	0.0408	8.73	4.84	1.13	0.720	0.477	0.0547	4
(8)	1781	0.0840	16.8	10.04	2.31	1.47	1.22	0.0727	4
(9)	1786	0.0985	19.6	10.00	2.29	1.46	1.20	0.0611	5
(10)	1795	0.0681	13.5	5.56	1.27	0.810	0.550	0.0407	1
(11)	1852	0.0794	15.3	7.21	1.62	1.04	0.747	0.0490	8
(12)	1880	0.0771	14.7	7.77	1.74	1.11	0.817	0.0554	8
(13)	1898	0.106	19.9	9.66	2.15	1.37	1.10	0.0553	10
(14)	1966	0.155	28.4	11.33	2.48	1.58	1.36	0.0479	3
(15)	1976	0.0587	10.7	7.22	1.57	1.00	0.717	<u>0.0671</u>	6

Weighted Mean f = 0.0550

Cr I λ 4254

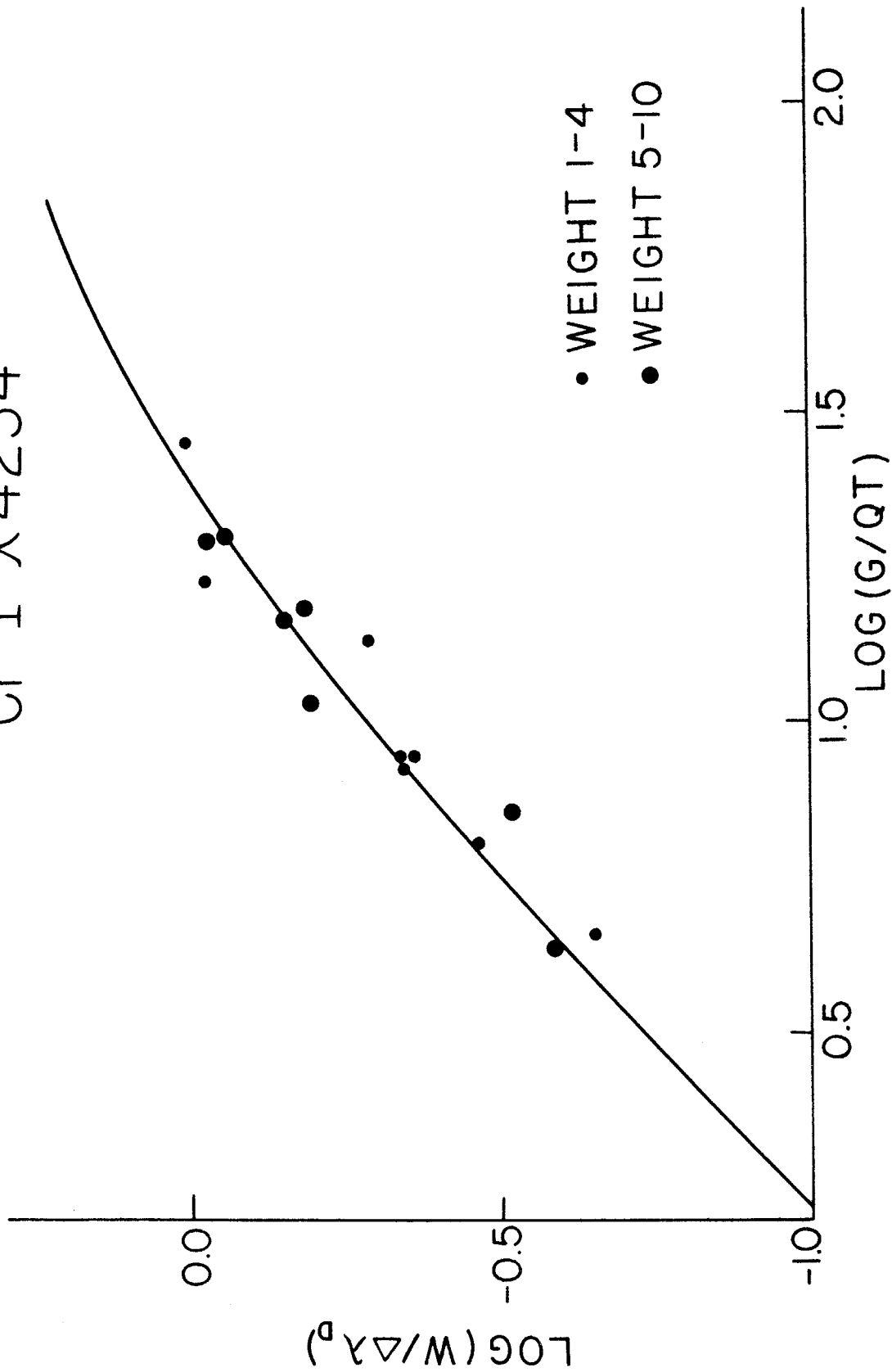


FIGURE 8

E. Errors

The average deviations given with the final results for each element indicate the magnitude of the scatter involved in the individual determinations of the absolute f -values. These average deviations range from about 8.5 percent of the mean value for copper and manganese to about 12.5 percent of the mean value for iron and chromium. Most of this scatter is the result of uncertainties in the equivalent width measurements (see Section IV H). Individual equivalent width measurements for weak lines (equivalent widths less than 0.005 Å.) may be in error by 25 or 30 percent, but for the stronger lines the equivalent width measurements are probably accurate to 15 or 20 percent. By averaging a series of equivalent width measurements made under constant experimental conditions, the uncertainty can probably be brought down to 10 or 15 percent. The accuracy of those data which have been assigned weights greater than 3 is in this range. An experimental technique that may improve the accuracy with which individual equivalent widths can be measured as well as allow measurements of very small equivalent widths will be briefly discussed in Section IV A.

Uncertainties in the deposit rate and temperature measurements are less than the uncertainties discussed above. Individual deposit rate measurements are probably accurate to 15 percent for very weak atomic beams (G less

than 0.1 micrograms per second) and accurate to 10 percent for stronger atomic beams. This accuracy is also improved when a number of measurements made under constant experimental conditions are averaged.

The temperature can be measured with an accuracy of at least 1 percent and dimensions of the atomic beam, height of the light beam above the atomic beam source, etc. can be determined with an accuracy of about 1 percent.

Most of the individually determined absolute f -values given in the tables of data already involve more than one equivalent width and deposit rate measurement. When these individual determinations are averaged according to the weights which have been assigned to them, they yield final absolute f -values which are probably accurate to ± 10 percent.

F. Summary

Table VI gives a summary of the absolute f -values that have been obtained for elements in the iron group up to the present time. Values in the column headed "Absorption Tube" are those obtained by King and his co-workers using the absorption tube method described in Section I. Absolute f -values given in parentheses in the "Absorption Tube" column were reported on the basis of earlier vapor pressure data, while all other numbers in that column are the revised absolute f -values based on the latest vapor pressure data. Values in the column headed "Atomic Beam" are the ones obtained in the present experiment. Absolute f -values given

TABLE VI
 Absolute f-Values for Lines in Spectra of the Iron Group

Element	λ	Terms	Absorption Tube	Atomic Beam	Others
Ti I	3355	$3F_3 - x^3G_4$		0.00036	van Stekeienburg and Smit (27)
		$4F_{4\frac{1}{2}} - z^3F_{4\frac{1}{2}}$		0.0028	
		$4F_{4\frac{1}{2}} - z^3F_{4\frac{1}{2}}$			
Ti II	3235	$4F_{4\frac{1}{2}} - z^3F_{4\frac{1}{2}}$			
Cr I	4254	$7S_3 - z^7P_4$	0.084(0.0122)	0.055	Huldt and Lagerqvist (7)
		$7S_3 - z^7P_4$			
	4275	$3 - 3$	0.067(0.0097)	0.043	0.00076
	4290	$3 - 2$	0.047(0.0068)	0.032	0.00055
	3579	$7S_3 - y^7P_4$			0.0028
3593	$3 - 3$			0.0022	
3605	$3 - 2$			0.0016	
Mn I	4031	$6S_2 - z^6P_3$		0.061	Huldt and Lagerqvist (7)
		$6S_2 - z^6P_3$			
	4033	$2 - 2$		0.034	0.046
4034	$2 - 1$		0.022	0.031	
Fe I	3720	$5D_4 - z^5D_5$	0.033(0.013)	0.032	Kopfermann and Wessel (11)
		$3 - 4$	0.032(0.013)		0.040
Ni I	3414	$3D_3 - z^3F_4$			
		$3D_3 - z^3F_4$			
	3524	$3D_3 - z^3P_4$	0.0133		
3461	$3D_3 - z^3F_4$	0.0093			
Cu I	3247	$4^2S_{\frac{1}{2}} - 4^2P_{1\frac{1}{2}}$	0.52(0.62)	0.31	Bates and Damgaard (8)
		$4^2S_{\frac{1}{2}} - 4^2P_{1\frac{1}{2}}$	0.27(0.32)	0.16	0.27

in the sixth column were obtained by investigators listed in the last column.

1. Titanium

The absolute f -values given by van Stekelenburg and Smit⁽²⁷⁾ for Ti I and Ti II were measured in emission using an arc into which TiO_2 was introduced. The temperature of the arc was determined from the CN bands, and the concentrations of Ti and Ti^+ in the column of the arc were evaluated from the rate of evaporation of the lower electrode, the convection velocity of the gas in the arc, and other data. In the opinion of van Stekelenburg and Smit, their absolute f -values are accurate only to an order of magnitude.

2. Chromium

The values obtained with the atomic beam for three resonance lines ($\lambda\lambda 4254, 4275, 4290$) of Cr I are 35 percent less than the revised values of Estabrook⁽⁶⁾ who used the absorption tube method. This indicates that further attention should be given to the absolute f -values of this important element in order to put the relative measurements of Hill⁽¹⁵⁾ on a more reliable absolute scale. For example, other lines of Cr I can be investigated by the atomic beam method and such measurements may throw new light on the discrepancies which now exist. Also, a new analysis of the vapor pressure data for chromium is being carried out by Hultgren⁽²⁰⁾ and results of this analysis may modify

Estabrook's values.

Since the absolute f-values given Huldt and Lagerqvist⁽⁷⁾ for this element are far less than those obtained by either of the other methods, it is not likely that they are reliable.

3. Manganese

In the case of the strongest line of Mn I, λ 4031, the absolute f-value obtained in the present experiment and that reported by Huldt and Lagerqvist⁽⁷⁾ agree very well. The agreement is not quite so good, however, for the other two lines of this triplet. Because of the weaknesses already pointed out in the method used by Huldt and Lagerqvist (see Section V D), it is believed that the absolute f-values obtained here are the more reliable.

4. Iron

If the most recent vapor pressure data on iron is taken to be the most reliable, then the revised absolute f-value (0.033) which King⁽⁴⁾ finds for the resonance line λ 3720, using the absorption tube method, agrees very well with the value (0.032) obtained with the atomic beam. This might indicate that the higher value (0.043) reported by Kopfermann and Wessel⁽¹¹⁾ is incorrect. However, the atomic beam method of Kopfermann and Wessel, though somewhat different from that used here, should give reliable values. Thus, it remains an open question for the present as to why absolute f-values of the iron resonance line obtained

by these different techniques do not agree.

5. Nickel

So far only the absorption tube method has been used for absolute f -value measurements on nickel. These measurements were made by Estabrook^(5,6) using the vapor pressure data of Johnston and Marshall.⁽²⁸⁾ More recent vapor pressure data by Hultgren⁽²⁰⁾ agree very well with that of Johnston and Marshall and leave Estabrook's published values for absolute f -values of nickel unchanged.

6. Copper

Absorption tube measurements by King and Stockbarger,⁽³⁾ and the most recent vapor pressure data of Hultgren,⁽²⁰⁾ yield an absolute f -value for the strongest line of Cu I ($\lambda 3247$) which is 1.67 times as large as that obtained by the atomic beam method. Since copper is one of the best behaved elements in both of these experiments, and since its vapor pressure seems to be well determined, this large discrepancy in the absolute f -value is surprising. For a time it was thought that the presence of the copper molecule Cu_2 in the atomic beam might be responsible for the difference. However, on the basis of experiments discussed in Section V A it was concluded that this effect was negligible. All other investigations of sources of error in the atomic beam failed to reveal any significant difficulties, and as Figure 4 shows, measurements made over a wide range of

line strengths gave very consistent results. Thus, an explanation for the discrepancy is not apparent from the standpoint of the atomic beam experiment.

Absolute f -values for the resonance lines of Cu I have been theoretically calculated by Bates and Damgaard.⁽⁸⁾ These calculations are based on a general expression for the transition integral which can be derived if the departure of the potential of an atom from its asymptotic Coulomb form is neglected. These theoretical absolute f -values are in much better agreement with the experimental values obtained by the absorption tube method than with the values obtained in the present experiment. However, it is quite possible that perturbations caused by the closed-shell electrons in the complex copper atom may make the theoretical calculations incorrect for copper. Therefore, the excellent agreement between the theoretical and absorption tube results may be fortuitous.

VI. SUGGESTIONS FOR FURTHER RESEARCH

A. Experimental Techniques

1. Photoelectric Measurements

If the atomic beam method described here is to be extended to other elements of astrophysical interest, it will be necessary to devise a method for measuring weaker absorption lines than have yet been measured. It seems very unlikely that the photographic process can be used for measurements on lines whose equivalent widths are less than 0.002 Angstroms, but a special photoelectric process could possibly measure lines an order of magnitude weaker than this. Circuits and techniques for such a process are being investigated.

2. Beam Density Indicator

One of the greatest difficulties encountered in the atomic beam experiment is the maintenance of a constant atomic beam density. Even when the temperature is well controlled, the beam density may still vary due to changes in the evaporating sample. These variations can usually be detected by a careful study of the recorder tracings after the run has been completed, but better data could be obtained if changes in the atomic beam density were immediately detectable.

Instantaneous detection of changes in the density of the atomic beam might be accomplished by suspending a light metal vane on a quartz fiber at one edge of the atomic beam. By shielding one half of the vane and allowing the other half to collect atoms from the beam, the torsion of the fiber, as indicated by a light beam and mirror arrangement, could be used to register the horizontal component of momentum of the depositing atoms. The weight of the beam deposit on the vane can be made negligible in comparison with the total weight of the vane, and thus the vane should hold a fixed position so long as the atomic beam density and velocity distribution remain constant. Spectrographic exposures and deposit rate measurements would then be made only at those times when the indicator showed that no significant changes were taking place in the beam.

Though simple in principle, such an indicator would probably require delicate instrumentation, a means of damping, and considerable testing.

B. Iron Group Elements

Davis⁽¹²⁾ has discussed the possibilities for making successful absolute f-value measurements on the resonance lines of the iron group elements, scandium, titanium, vanadium, chromium, manganese, iron, cobalt, nickel, and copper, using the atomic beam method. In addition to the elements copper, manganese, iron, and chromium for which absolute

f-values have now been obtained, cobalt appears to be a good prospect for investigation. This element melts at a temperature of 1495° C. and an exploratory plate taken by Davis has shown that an effective beam can be obtained at a temperature of 1800° C. Cobalt has a complex ground state, a 4F , which means that the lowest sub-level will be somewhat depopulated at the temperatures needed for an effective beam, but the strongest lines arising from this level have equivalent widths large enough for measurement in spite of this difficulty.

Scandium would be an important element to investigate because its relative abundance helps to define the iron peak of the abundance curve. However, this element has not yet been isolated in the pure form and thus its absolute f-values cannot be measured by the atomic beam method.

Nickel is also an important element astrophysically and measurements of absolute f-values for three of its resonance lines have been made by the absorption tube method. (See Section V F.) To compare these measurements with atomic beam determinations would be of considerable interest, but the absorption lines formed in the atomic beam may be too weak for measurement with the present apparatus. If this proves to be the case, two things might be tried. First, additional traversals of the light beam through the atomic beam might be attempted in order to increase the effective absorbing path. Second, a photoelectric technique might be used to measure the equivalent

widths of lines weaker than can be measured by the photo-electric process.

For several reasons titanium and vanadium appear to be dubious prospects for absolute f-value measurements using the atomic beam method. First, the high melting points of titanium (1800° C.) and of vanadium (1710° C.) indicate that in all probability an effective beam cannot be produced without going to temperatures beyond the working range of the present equipment. Second, titanium is especially difficult to hold when in the molten state because of its strong tendency to react with other elements. (See Reference 29.) And third, each of these elements has a complex ground state which means that the atoms in the beam will be distributed over the sub-levels of this state in such a way that many of them cannot contribute to any one transition. This is also a difficulty in the case of cobalt and nickel, but because of the lower melting points, strong atomic beams of these two elements can be produced to compensate for this depletion in the atomic beam of effective absorbing atoms. Because of the astrophysical importance of titanium and vanadium, it is hoped that these obstacles can be overcome and that reliable absolute f-values will eventually be obtained for these elements.

C. Other Elements

Though the apparatus described in this report was originally designed for absolute f-value measurements on

the iron group elements, it can also be used for certain other elements having similar properties. Because the relative abundances of some of these elements are of astrophysical interest, it would be of value to know something of their absolute f -values from experimental measurements, even if the values could not be determined to high accuracy. Though no attempts have yet been made in this laboratory to investigate these elements, a review of their properties and spectra indicate the following possibilities for making successful absolute f -value measurements by the atomic beam method.

1. Magnesium

Magnesium melts at 651° C. and boils at 1110° C.; an effective beam could probably be produced at temperatures below 1000° C. The reaction of the metal with other materials would probably not be a problem, particularly if a ceramic boat were used. The ground state of Mg I is a 3^1S state and the spectral line of astrophysical interest is the intersystem line $\lambda 4571$ ($3^1S_0-3^3P_1^0$). This line, as well as lines in the infra-red, have been used for solar abundance determinations. It is doubtful whether the intersystem line would be sufficiently strong to permit an atomic beam measurement, but the absolute f -value for the resonance line $\lambda 2852$ ($3^1S_0-3^1P_1^0$) might be successfully measured by this method. Because of the enormous difference in the strengths of the resonance and intersystem

lines, it is questionable whether the relative f-values of these lines could be measured with a King furnace.

2. Aluminum

Aluminum is of astrophysical interest and seems to be a good prospect for absolute f-value measurements using the atomic beam method. It melts at 659.7° C. and boils at 2057° C.; an effective beam could probably be obtained at temperatures somewhat above 1000° C. Holding this metal in the molten state should present no serious difficulties. The ground state of Al I is a doublet (3^2P) giving rise to the resonance lines $\lambda 3944$ and $\lambda 3962$ which are observed in astrophysical sources. These lines are in a suitable region for absolute f-value measurements by the atomic beam method and presumably they could be produced with sufficient strength for accurate measurement. The spectral lines of Al I exhibit fairly large hyperfine structure. Fortunately, this structure has been experimentally measured and analyzed for the resonance lines by Jackson and Kuhn.⁽³⁰⁾ Therefore, it could be taken into account in the absolute f-value measurements.

3. Silicon

For astrophysical reasons, it would be desirable to have experimentally determined absolute f-values for some spectral lines of silicon. Unfortunately, this element does not appear to be one which can be investigated by the

atomic beam method. Because silicon reacts readily with other elements, it would no doubt be difficult to hold in the molten state. Even more serious is the fact that the resonance lines of Si I are in the λ 2200-2500 region and therefore are practically inaccessible for accurate measurements.

4. Calcium

The spectral lines of calcium are some of the most prominent in solar and stellar spectra. The strongest of these lines are produced by Ca II, but strong lines of Ca I are also observed. A project is now under way to determine relative f-values for many of the lines of Ca I and it would be very desirable to have these values on an absolute scale. However, the strong tendency for calcium to react with other elements makes absolute f-value determinations by any technique extremely difficult. Attempts made by Estabrook⁽³¹⁾ to hold calcium in an absorption tube failed because the calcium reacted with the quartz tube making it opaque. In an atomic beam measurement there would be the difficulty of making a boat which would not combine with calcium. There is also the problem of obtaining a pure sample of the metal and introducing it into the furnace before an oxide can form. In spite of these difficulties, however, more attempts will be made to measure absolute f-values for Ca because of its astrophysical importance. If the atomic beam method is used, it is probable

that only the very strong resonance line $\lambda 4227$ ($4^1S-4^1P^0$) can be investigated. This is unfortunate because the relative strength of this line as compared to the intersystem line $\lambda 6573$ ($4^1S-4^3P^0$), and to other lines of astrophysical interest, is not well established. Nevertheless, an experimental measurement of the absolute f -value for the resonance line $\lambda 4227$ would be valuable for checking theoretical determinations and for putting all f -values for Ca I on an absolute scale at some time in the future when this line is tied in with the weaker lines by reliable relative f -value measurements.

5. Zirconium

Of the heavier elements, zirconium is of some astrophysical interest because its spectrum is rich with lines throughout the visible and ultra-violet regions. Zirconium has a triplet ground state, a^3F , and lines arising from this ground state are found in all parts of the spectrum. Apparently, the strongest of these lines are located in the 3500-3700 A wave length region. However, it will be difficult to make absolute f -value measurements on zirconium by the atomic beam method because of the high melting point (1900° C.) of this element. In order to produce measurable absorption lines, temperatures over 2000° C. will no doubt have to be reached.

6. Silver

Silver is probably the most promising of the heavier elements for absolute f-value measurements using the atomic beam method. It melts at 961° C. and boils at 1950° C., so that the temperature range in which an effective beam can most likely be produced is ideal. Holding silver in the molten state should not be difficult. The ground state of Ag I is $5s^2S$ and from this state two strong lines $\lambda 3281$ and $\lambda 3383$ ($5^2S_{\frac{1}{2}}-5^2P_{\frac{3}{2},\frac{1}{2}}^{\circ}$) are found in the ultra-violet region. Absolute f-values for these two lines should not be difficult to measure, and, if desired, relative f-values for these and weaker lines could probably be measured using a King furnace.

7. Barium

Barium is one of the few heavy elements for which an absolute f-value has been experimentally determined. This measurement was made by Wessel⁽¹⁰⁾ using an atomic beam technique; he obtained an absolute f-value of 2.10 for the resonance line $\lambda 5535$ ($6^1S-6^1P^{\circ}$) of Ba I. Barium has a rather low melting point (850° C.) and Wessel was able to produce an effective beam in the temperature range of 548 to 621° C., that is, with the barium in the solid state. If an effective beam of barium could also be produced in the apparatus here without melting the element, the problem of holding this active element would be greatly simplified.

An attempt will be made in the near future, using the present equipment, to measure the absolute f -value of the Ba I line investigated by Wessel. Such a measurement will serve as a further check on the results obtained by these slightly different experiments.

8. Lead

Relative abundance determinations for elements in the atmosphere of the sun show an anomalously high abundance for lead as compared with the relative abundance of this element in meteorites. Theoretical estimates of the absolute f -values for lines in lead had to be used in these abundance determinations since no experimental data were available. Theoretical estimates of absolute f -values for heavy, complex atoms such as lead are questionable, and therefore it would be of value to measure the absolute f -values of such elements experimentally. Lead should not be difficult to hold in the molten state and, because of its low melting point (327° C.), high temperatures would not have to be used to produce a beam. A thermocouple would no doubt have to be used for temperature measurement and control. Neutral lead has a triplet ground state, $6p^3P$, the sub-levels of which are widely separated. The second and third sub-levels of this ground state lie 0.97 and 1.31 e.v. respectively above the lowest level. The line of greatest astrophysical interest lies at $\lambda 4057$ and arises from the highest sub-level of the ground state.

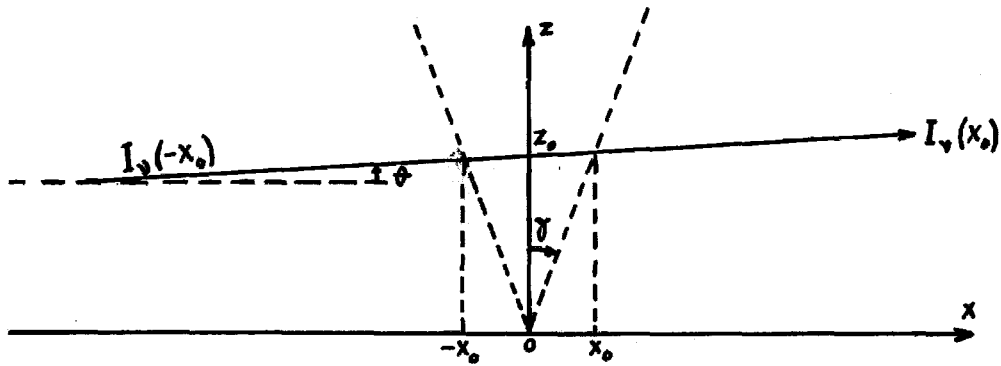
Probably the only line which could be investigated in the atomic beam apparatus would be the line $\lambda 2833$ ($6p^3P_0 - 7s^3P_1^0$) which arises from the lowest level. If successful absolute f-value measurements could be made on this resonance line, $\lambda 2833$, then relative f-value determinations could supposedly be made to relate its strength to that of other lines of astrophysical interest.

APPENDIX

VII. THEORY FOR MULTIPLE LIGHT BEAM

Davis⁽¹²⁾ has developed in detail the theory underlying the present experiment. The essential part of this theory is the development of an expression for the transmitted intensity of a light beam as it emerges from the atomic beam. Since the density and velocity distribution of the atomic beam are not uniform, the expression for the transmitted light intensity involves an integration along its path through the atomic beam. The transmitted intensity is also a function of the wave length of the light, and a second integration must be carried out over all wave lengths to obtain the equivalent width of the absorption line.

Davis considered only the case of a horizontal traversal where the z-coordinate of the light beam has the constant value, z_0 . In the present arrangement of equipment, however, it is necessary to consider a light path which makes a small angle with the horizontal axis, since even numbered traversals are turned slightly upward by one of the concave mirrors (see Figure 1). In the derivation of an expression for the transmitted intensity under such conditions, a rectangular coordinate system is set up with the origin at the atomic beam source, as illustrated in the following figure.



The quantities $-x_0$ and x_0 are the x -coordinates of the light beam as it enters and leaves the atomic beam, and the quantity z_0 is the vertical height of the light beam above the origin at the center of the atomic beam. The light beam is considered sufficiently narrow that variations in the y -direction can be neglected, and it is considered to be of negligible thickness in the z -direction.

When light of a given frequency passes through the atomic beam from $-x_0$ to x_0 , the transmitted intensity is

$$I_v(x_0) = I_v(-x_0) \exp - \int_{-x_0}^{x_0} N(x,z) \alpha_v(x,z) dx \quad (19)$$

The integrand in the second term of this equation is the number of atoms per unit volume at the point (x,z) in the atomic beam multiplied by the absorption coefficient per atom. Davis shows that this product is given by

$$N(x,z) \alpha_v(x,z) = \frac{2C'za}{\pi x^3} \int_0^{\infty} \frac{\eta^2 e^{-\eta^2(1+z^2/x^2)}}{a^2 + (\omega - \eta)^2} d\eta \quad \text{for } x > 0$$

$$N(x,z) \alpha_v(x,z) = \frac{-2C'za}{\pi x^3} \int_0^{\infty} \frac{\eta^2 e^{-\eta^2(1+z^2/x^2)}}{a^2 + (\omega + \eta)^2} d\eta \quad \text{for } x < 0 \quad (20)$$

where

$$C' = \frac{G}{Q'T} f,$$

G is the deposit rate of atoms striking the balance pan,

T is the absolute temperature,

f is the absolute f-value for the line in question,

$$Q' = 3.28 \times 10^{-3} \frac{f^2}{\lambda_0 (f^2 + b^2)},$$

f is the radius of the circular opening which defines the deposit on the balance pan,

b is the height of this opening above the source,

λ_0 is the wave length of the center of the line,

$$a = \frac{\lambda_0}{4\pi} \Gamma \beta,$$

Γ is the natural damping constant of the line,

$$\beta = \sqrt{\frac{M}{2RT}}$$

$$\eta = u\beta$$

u is the velocity of the absorbing atoms in the x-direction,

$$\omega = \frac{\lambda - \lambda_0}{\lambda_0} \beta c, \text{ and}$$

λ is the wave length of the light.

From the figure it is easy to see that z can be expressed as a linear function of x in the form

$$z = z_0(1 + \epsilon x) \quad (21)$$

where $\epsilon = \frac{\tan \theta}{z_0}$, θ being the angle which the light beam makes with the horizontal axis. In the optical arrangement used here, $\tan \theta = 0.026$, z_0 is between 2 and 3 cm., and x_0 is around 2 cm. Thus, x_0 is approximately 0.02, so

that ϵx can be considered small compared to 1 throughout the integration. Hence, to a good approximation,

$$z^2 = z_0^2(1 + 2\epsilon x).$$

Substitution of these expressions for z and z^2 into equation 20 and integrating from $-x_0$ to x_0 gives

$$\int_{-x_0}^{x_0} N(x) \alpha_v(x) dx = \frac{2C_1 z_0 a}{\pi} \int_0^{\infty} \left[\frac{1}{a^2 + (\omega - \eta)^2} + \frac{1}{a^2 + (\omega + \eta)^2} \right] \left[\int_0^{x_0} \frac{(1 + \epsilon x) \eta^2}{x^3} e^{-\eta^2 \left(1 + \frac{z_0^2 (1 + 2\epsilon x)}{x^2} \right)} dx \right] d\eta \quad (22)$$

The integration over x can be carried out by making the following change of variable. Let

$$u = -\eta^2 \left(1 + \frac{z_0^2 (1 + 2\epsilon x)}{x^2} \right) \quad (23)$$

$$du = 2\eta^2 z_0^2 \left(\frac{1 + \epsilon x}{x^3} \right) dx$$

Then,

$$\int_0^{x_0} \frac{\eta^2 (1 + \epsilon x)}{x^3} e^{-\eta^2 \left(1 + \frac{z_0^2 (1 + 2\epsilon x)}{x^2} \right)} dx = \frac{1}{2z_0^2} \int_{-\infty}^{u(x_0)} e^u du = \frac{1}{2z_0^2} e^{u(x_0)}$$

(24)

$$\begin{aligned}
 u(x_0) &= -\eta^2 \left(1 + \frac{z_0^2 (1+2\epsilon x_0)}{x_0^2} \right) \\
 u(x_0) &= -\eta^2 \left(\frac{x_0^2 + z_0^2}{x_0^2} + \frac{2\epsilon z_0^2}{x_0} \right) \\
 u(x_0) &= -\eta^2 \left(\csc^2 \gamma + \frac{2\epsilon z_0^2}{x_0^2} \right)
 \end{aligned}
 \tag{25}$$

where γ is the half-angle of the atomic beam.

The half-angle of the atomic beam, γ , is about 40° so that the $\csc^2 \gamma$ is about 2.4. Using the previously mentioned values for ϵ , x_0 , and z_0 , the quantity $2\epsilon z_0^2/x_0$ is about 0.064. Thus, the correction term, $2\epsilon z_0^2/x_0$, in the expression for $u(x_0)$ is only about 2.7 percent of the main term, $\csc^2 \gamma$. This corresponds to a factor of less than 1 percent in γ , which is considerably less than the probable error made in the actual measurement of γ . Thus, an insignificant error is made if the correction term is neglected. This corresponds, of course, to neglecting the fact that the light beam passes through the atomic beam at a small angle of inclination rather than horizontally, and it greatly simplifies the expressions needed for the calculation of absolute f-values. Correction terms can be calculated, but they are not needed so long as the angle of inclination, θ , is less than 2° .

In the present optical arrangement θ has a value of about 1.5° . For such an angle the approximation is valid and the integration over x in equation 24 gives

$$\frac{1}{2z_0^2} e^{-\eta^2 \csc^2 \gamma} \quad (26)$$

Equation 22 then becomes

$$\int_{-x_0}^{x_0} N(x) \alpha_{\nu}(x) dx = \frac{C'a}{\pi z_0} \int_0^{\infty} \left[\frac{1}{a^2 + (\omega - \eta)^2} + \frac{1}{a^2 + (\omega + \eta)^2} \right] e^{-\eta^2 \csc^2 \gamma} d\eta \quad (27)$$

With the approximation that all traversals of the light beam pass through the atomic beam horizontally, it is easy to generalize equation 19 to cover the case of multiple traversals. Let x_1, x_2, \dots, x_n be the x-coordinates of the individual light beam traversals as they emerge from the atomic beam. The integrations over x can be separated into a series of integrals covering each traversal, so that equation 19 becomes

$$I_{\nu}(x_n) = I_{\nu}(-x_1) \exp - \left[\int_{-x_1}^{x_1} N_1 \alpha_1 dx + \int_{-x_2}^{x_2} N_2 \alpha_2 dx + \dots + \int_{-x_n}^{x_n} N_n \alpha_n dx \right] \quad (28)$$

Each integral over x in the exponent of equation 28 can be evaluated as already shown; hence, by equation 27 the exponent is

$$\frac{C'a}{\pi} \left(\frac{1}{z_1} + \frac{1}{z_2} + \dots + \frac{1}{z_n} \right) \int_0^{\infty} \left[\frac{1}{a^2 + (\omega - \eta)^2} + \frac{1}{a^2 + (\omega + \eta)^2} \right] e^{-\eta^2 \csc^2 \gamma} d\eta \quad (29)$$

where z_1, z_2, \dots, z_n are the heights above the origin of the individual traversals. This corresponds to the expression given by Davis for the exponent except that his quantity C is now given by

$$C'(1/z_1 + 1/z_2 + \dots + 1/z_n). \quad (30)$$

Nothing further is changed in the equivalent width derivation, and Davis' procedure can be followed step by step to the final expression. This expression is

$$\frac{W}{\Delta \lambda'_D} = \frac{W}{\Delta \lambda_D \sin \gamma} = \sqrt{\pi} \sum_{n=1}^{\infty} \frac{C^n (-1)^{n+1}}{n! \sqrt{n}} \quad (31)$$

where

W is the equivalent width of the line,

$\Delta \lambda_D$ is the doppler width of the line,

γ is the half-angle of the atomic beam, and

$$\begin{aligned} C &= C'(1/z_1 + 1/z_2 + \dots + 1/z_n) \\ &= \frac{Gf}{T} \frac{1/z_1 + 1/z_2 + \dots + 1/z_n}{Q'} \end{aligned} \quad (32)$$

The last factor in the expression for C can be defined as $1/Q$ where

$$Q = \frac{Q'}{1/z_1 + 1/z_2 + \dots + 1/z_n}$$

$$Q = 3.28 \times 10^{-3} \frac{f^2}{f^2 + b^2} \frac{1}{\lambda_0} \frac{1}{1/z_1 + 1/z_2 + \dots + 1/z_n}$$

(33)

This general expression for Q reduces to the usual expression for Q as given by equation 5 when only a single beam is used.

REFERENCES

- (1) King, R. B., and King, A. S., Astrophys. J., 82, 377 (1935).
- (2) King, R. B., and King, A. S., Astrophys. J., 87, 24 (1938).
- (3) King, R. B., and Stockbarger, D. C., Astrophys. J., 91, 488 (1940).
- (4) King, R. B., Astrophys. J., 95, 78 (1942).
- (5) Estabrook, F. B., Astrophys. J., 113, 684 (1951).
- (6) Estabrook, F. B., Astrophys. J., 115, 571L (1952).
- (7) Huldt, L., and Lagerqvist, A., Arkiv for Fysik, 5, 91 (1952).
- (8) Bates, D. R., and Damgaard, A., Phil. Trans. Roy. Soc. (London), 242A, 101 (1949).
- (9) Landolt-Börnstein, Zahlenwerte u. Funktionen, b. 1, Springer, Berlin (1950).
- (10) Wessel, G., Z. f. Phys., 126, 440 (1949).
- (11) Kopfermann, H., and Wessel, G., Z. f. Phys., 130, 100 (1951).
- (12) Davis, M. H., Thesis, Calif. Inst. of Tech. (1955).
- (13) Unsold, A., Physik der Sternatmosphären, Springer, Berlin (1938).
- (14) Aller, L. H., Astrophysics, v. 1, Ronald, New York (1935).
- (15) Hill, A. J., Thesis, Calif. Inst. of Tech. (1950); J. Op. Soc. Am., 41, 315 (1951).
- (16) Heavens, O., Optical Properties of Thin Solid Films, Academic Press, New York (1955).
- (17) Handbook of Chem. and Phys., 37th ed., 2701, Chem. Rubber Co. (1956).
- (18) Harteck, P., Z. f. Phys.-Chem., 134, 1 (1928).

- (19) Hersh, H. N., J. Am. Chem. Soc., 75, 1529 (1953).
- (20) Hultgren, R., Selected Values for the Thermodynamic Properties of Metals and Alloys (1955) (Unpublished)
- (21) Kleman, B., and Lindkvist, S., Arkiv för Physik, 8, 333 (1954).
- (22) White, H. E., Introduction to Atomic Spectra, 440, McGraw-Hill, New York (1934).
- (23) White, H. E., and Ritschl, R., Phys. Rev., 35, 1146 (1930).
- (24) Carter, W. W., Phys. Rev., 76, 962 (1949).
- (25) Marshall, A. L., Dornte, R. W., and Norton, F. J., J. Am. Chem. Soc., 59, 1161 (1937).
- (26) Edwards, J. W., Johnston, H. L., and Ditmars, W. E., J. Am. Chem. Soc., 73, 4729 (1951).
- (27) van Stekelenburg, L. H., and Smit, J. A., Physica, 14, 189 (1948).
- (28) Johnston, H. L., and Marshall, A. L., J. Am. Chem. Soc., 62, 1382 (1946).
- (29) Hampel, C. A., Rare Metals Handbook, 455-482, Reinhold, New York (1954).